French Air and Space Force Academy

End of studies thesis

eVTOLs' paths in urban environment for rescue missions

Thesis realized by the SLT AGOUDJIL–ELSPASS Célian

Under the supervision of the Dr WANG Zihao

Juin 2024

Plagiarism integrity statement

I hereby certify that :

- I am the author of this work.
- I have attributed and cited all borrowed content according to expected methodological practices.

Name : AGOUDJIL–ELSPASS Surname : Célian

Date : 12/06/2024 Signature :

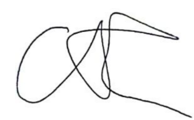

Résumé

Dans un contexte où la population mondiale ne cesse d'augmenter, les agglomérations s'étendent de plus en plus, augmentant divers risques, qu'ils soient environnementaux, liés à la santé qui se dégrade, ou à la complexification du trafic qui mène à plus d'accidents en tous genres en milieu urbain. C'est pourquoi, grâce aux avancées technologiques, les eVTOLs (drones autonomes et électriques) apparaissent comme une solution pour pallier les risques croissants que représente la complexification du trafic routier, cela en allant chercher les victimes puis en les ramenant en lieu sûr.

Pour ce faire, les trajectoires des eVTOLs seront examinées en deux dimensions, en tenant compte des obstacles statiques dus au milieu urbain et des autres eVTOLs également en mission, avec lesquels il ne faudra pas entrer en collision et dont l'objectif sera de coordonner leurs trajectoires entre eux en fixant des règles de priorité.

Pour cela, un algorithme naïf sera réalisé, permettant à l'eVTOL d'aller chercher la victime en esquivant les obstacles statiques puis de ramener la victime aux urgences, mais sans être optimisé. Ensuite, cet algorithme sera comparé avec un autre plus performant où la trajectoire est optimisée, montrant des résultats prometteurs sur certains aspects. Par la suite, il sera question d'étudier le trafic entre plusieurs eVTOLs qui doivent aller secourir plusieurs victimes, sans entrer en collision les uns avec les autres.

Dans l'ensemble, les résultats montreront un taux de réussite très élevé tout en mettant en lumière ce qui peut être optimisé et amélioré, ce qui invitera à des recherches plus poussées afin d'implémenter ces algorithmes aux modèles en cours de développement, comme le modèle Vertiia développé actuellement à l'aéroport de Bankstown à Sydney.

Abstract

In a context where the global population continues to increase, urban areas are expanding more and more, heightening various risks, whether they are environmental, health-related due to deteriorating conditions, or traffic-related, leading to more accidents of all kinds in urban environments. This is why, thanks to technological advancements, eVTOLs (electric and autonomous drones) appear as a solution to mitigate the growing risks posed by the complexity of road traffic, by rescuing victims and bringing them to safety.

To achieve this, the trajectories of eVTOLs will be examined in two dimensions, taking into account static obstacles in the urban environment and other eVTOLs on similar missions with which they must avoid collisions, aiming to coordinate their trajectories by establishing priority rules.

A naïve algorithm will be developed, allowing the eVTOL to rescue the victim by avoiding static obstacles and then transporting the victim to the emergency services without optimization. This algorithm will then be compared with a more efficient one where the trajectory is optimized, showing promising results in certain aspects.

Subsequently, the focus will shift to studying the traffic among multiple eVTOLs that need to rescue several victims without colliding with each other.

Overall, the results will show a very high success rate while highlighting what can be optimized and improved, encouraging further research to implement these algorithms into models under development, such as the Vertiia model currently being developed at Bankstown Airport in Sydney.

List of figures

List of tables

Acknowledgments

I would like to express my sincere gratitude to Mr. Wang, a doctor at the University of Sydney, for his assistance. He played a crucial role in facilitating the logistics of my visit and provided invaluable scientific and personal support to ensure the success of this internship. I am truly grateful for his guidance.

I would also like to thank Mr. Kolb for his guidance and his desire to see me progress in my work despite the initial logistical challenges.

My appreciation also extends to all of my family and my friends for their support.

Finally, I wish to pay tribute, through this thesis, to Yixuan Cheng, a student at the University of Sydney, who was tragically murdered in an attack on April 13, 2024.

Table of contents

1 Introduction

1.1 Context

With the continuous growth of the global population, major urban areas are experiencing rapid expansion. This increasing urbanization creates an environment where traffic becomes more complex and dense, increasing the risk of accidents of daily life. Urban infrastructures are facing mounting pressure, leading to significant challenges in traffic management and road safety. This situation contributes to the rise in everyday accidents and incidents related to urban traffic. The increasing number of vehicles and pedestrians in urban areas creates scenarios prone to various accidents, necessitating innovative solutions to prevent these risks and ensure public safety.

At the same time, technological advances have enabled us to invent ever more efficient aircraft, with greater carrying capacity, higher speeds and optimised materials. From drone to helicopter, the latest development is the eVTOL, which represents a global market worth several billion dollars and which continues to expand all over the world.

Regarding the technological field, the emergence of electric vertical take-off and landing (eVTOL) aircraft is opening up possibilities for new urban air mobility services, aligning closely with the focus on managing eVTOLs traffic in urban environment for rescue missions. eVTOLs can enable on-demand, rapid transportation between urban vertiports situated within city centers. However, their safe integration in high densities requires addressing significant challenges posed by confined urban airspaces, a key aspect to consider in devising effective traffic management strategies.

Even though current urban drone traffic studies provide a baseline, eVTOLs are of different scale and dynamics, which required coming up with new solutions specific to them, as addressed directly in this thesis. Simultaneously, the results suggest that knowledge brokering can be a two-way exchange of ideas between the urban drone management domain, further exemplifying the interconnected nature of the aerial traffic management research, and its applicability over multiple verticals.

In addition to facilitating urban mobility, eVTOLs possess the potential to support and enhance search and rescue operations, particularly in accessing remote or inaccessible areas where traditional transportation methods may be limited. Recent incidents, such as natural disasters or medical emergencies such as the crisis of COVID19, underscore the importance of integrating eVTOLs into rescue missions, providing rapid and efficient aerial support to save lives and mitigate damages.

1.2 Global issue

How can the traffic management of eVTOLs in urban environments be ensured for rescue missions ?

1.3 Objectives

The objectives of this thesis are listed below in logical order and increasing difficulty :

1. Create a credible environment and scenario for saving lives in an urban setting.
2. Develop a naive algorithm implementable in an eVTOL so that it can autonomously complete its mission by avoiding obstacles commonly found in urban areas.
3. Compare this naive algorithm with another optimized algorithm to assess its credibility.
4. Extend this idea to a more complex scenario involving multiple eVTOLs rescuing multiple targets.
5. Apply the algorithm to a concrete case study.

1.4 Thesis structure

The paper is organized as follows :

- Section 1 provides an introduction to understand the scope of the subject.
- Section 2 provides a global literature review which enables to understand better the relevancy of the thesis.
- Section 3 describes the methodology used to answer properly the global issue.
- Section 4 provides results about the simulations made.
- Section 5 opens a discussion about the results obtained.
- Section 6 gives a conclusion detailing the contribution made to the thesis and how to expand the topic for future studies.
- Section 7 contains all the references used throughout the thesis.
- Section 8 provides the results of the simulations compiled on Excel and a link to access the code in addition to Youtube videos illustrating the simulations.

2 Literature review

2.1 General considerations

This section provides a broad overview air traffic issues in urban environment, especially for rescue missions in a context where the number daily life accidents rise exponentially due to the global rise of the population in the world.

2.1.1 Risks of accidents in expanding urban areas

According to the United Nations [1], global urbanization surpassed 50% in 2014, with North America, Europe, and Oceania leading since the 19th century. Rapid urbanization occurred in South and Central America during the 1960s-1980s, followed by explosive growth in Asia from the 1980s. By 2020, urban population constituted 56% globally, with North America at 26% above average. The UN predicts urbanization will rise to 60.4% by 2030, driven mostly by less developed regions like East Asia, South Asia, and Africa, notably India, China, and Nigeria contributing significantly [2].

Characteristic	2000 to 2005	2005 to 2010	2010 to 2015	2015 to 2020*	2020 to 2025*	2025 to 2030*	2030 to 2035*
Tokyo, Japan	0.67%	0.68%	0.21%	0.07%	0.19%	0.25%	0.31%
Delhi, India	3.50%	3.25%	3.25%	3.16%	2.70%	2.32%	2.14%
Shanghai, China	3.60%	3.50%	2.90%	2.84%	2.38%	1.51%	0.88%
Mexico City, Mexico	0.87%	0.87%	1.16%	0.41%	0.87%	1.16%	1.05%
Sao Paulo, Brazil	1.44%	1.45%	1.21%	1.08%	0.84%	0.71%	0.55%
Mumbai, India	1.33%	1.13%	1.13%	1.10%	1.58%	2.13%	2.14%
New York, United States	0.31%	0.31%	0.31%	0.17%	0.37%	0.82%	0.84%
Beijing, China	4.67%	4.71%	2.27%	2.10%	1.98%	1.44%	0.87%
Cairo, Egypt	2.15%	2.15%	2.15%	2.10%	1.98%	2.01%	2.21%
Dhaka, Bangladesh	3.63%	3.56%	3.56%	3.54%	3.20%	2.60%	2.13%

FIGURE 2.1 – Growth rate for the largest urban agglomerations worldwide from 2000 to 2035 [2]

Given that urban areas are expanding, road traffic is also increasing. Consequently, the risk of everyday accidents is proportional to the population growth. These accidents are often non-fatal but still require emergency response from rescue services. This can be challenging at times due to traffic congestion in large urban areas [3].

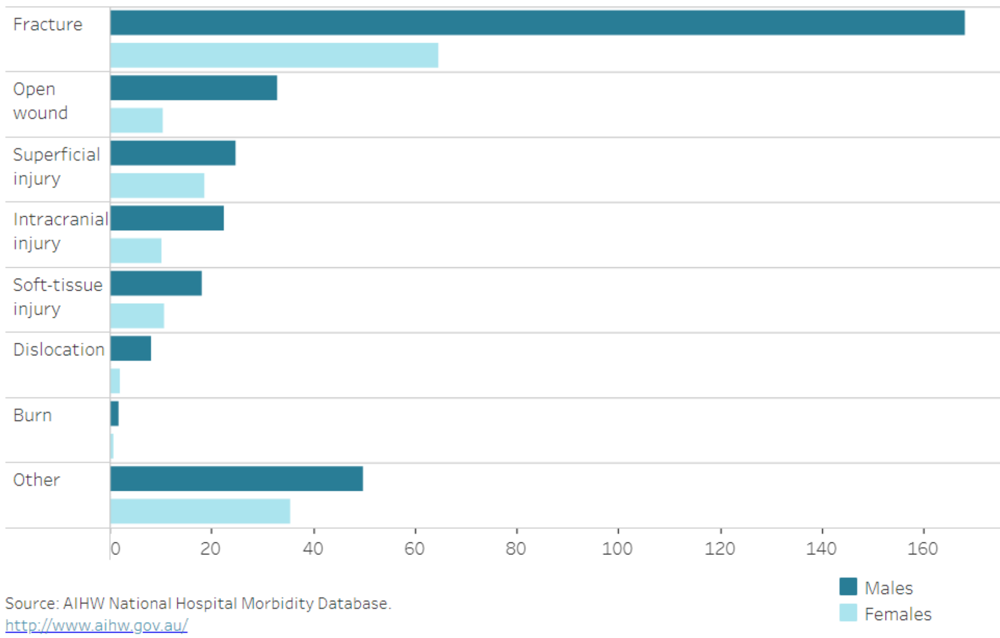

FIGURE 2.2 – Type of injuries caused by road accidents [3]

Moreover, everyday accidents sometimes involve medical reasons, such as the increasing prevalence of obesity worldwide, leading to a rise in cardiovascular diseases like heart attacks [4]. These situations require urgent interventions where every second counts to resuscitate the individual. This situation was further exacerbated during the COVID-19 crisis when ambulances had to retrieve patients from their homes to transport them to the intensive care unit. Around the world, tens of millions of people have been rescued at home, potentially saving them from death [5].

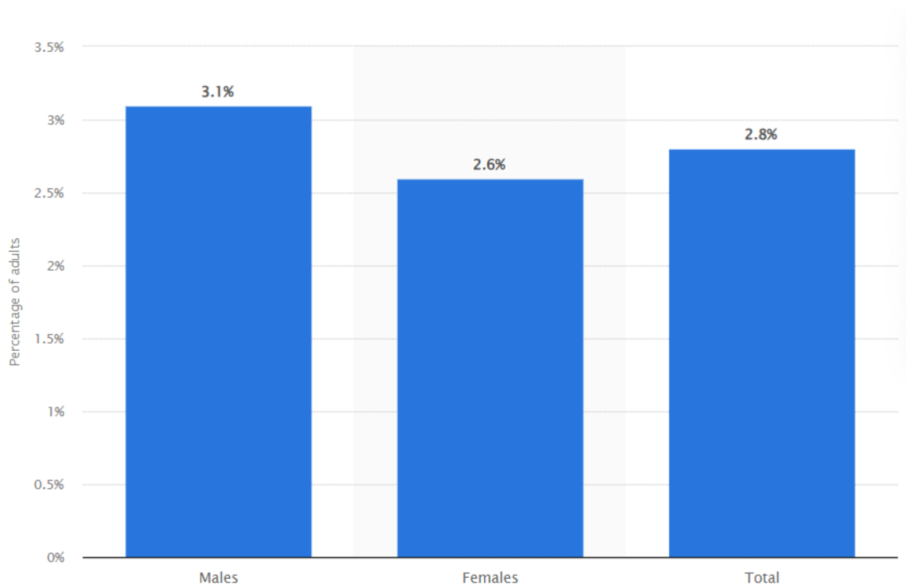

FIGURE 2.3 – Percentage of the US population who had a heart stroke in 2019 [4]

Similarly, climate change has led to a significant increase in natural disasters occurring across the globe. The overall rise in global temperatures has resulted in an increase in the number and intensity of wildfires [6]. Likewise, floods are expected to become more frequent, whether due to tsunamis or the melting of ice caps. Therefore, it is important to find ways to rescue people caught in such situations, especially where ambulances may be powerless due to extreme weather conditions.

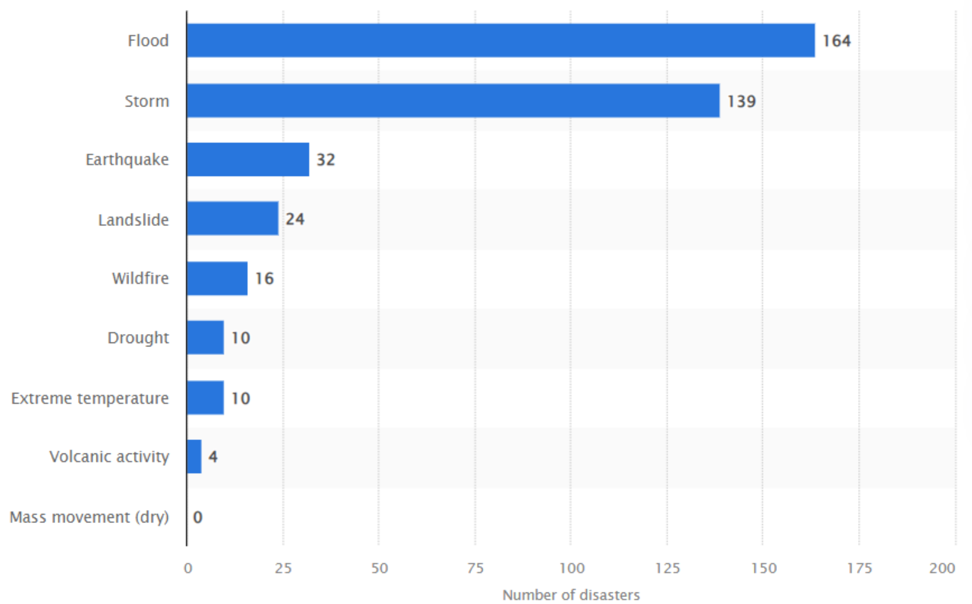

FIGURE 2.4 – Number of disasters per type. Photo from Statista

2.1.2 Air traffic management paradigms in confined spaces

Currently, the traditional air traffic management system employs different paradigms like positive control, self-separation, and free flight [7][8]. On one hand, positive control relies on air traffic controllers actively monitoring aircraft positions and communicating instructions to pilots [9]. This allows tight coordination but faces challenges in scaling to high air traffic densities [9]. On the other hand, self-separation delegates more responsibility to flight operators in maintaining safe distances from other aircraft based on onboard sensors and automation. It reduces controller workload but requires advanced avionics and pilot capability. Lastly, free flight aims to minimize external control and open airspace access by equipping operators for self-separation.

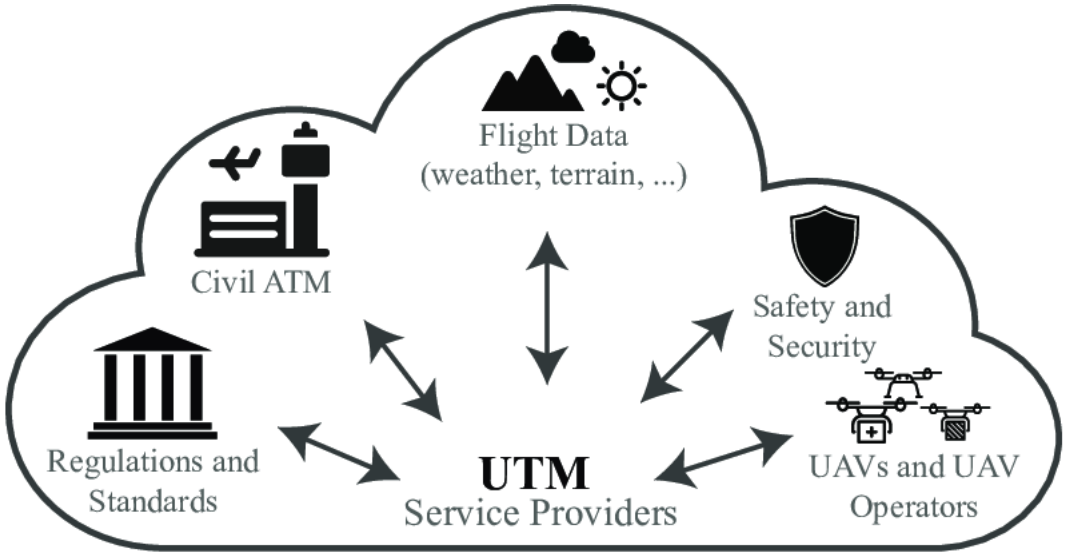

FIGURE 2.5 – Different actors implied in the air traffic management [7]

However, safety concerns exist about relying solely on decentralized operation in congested airspace. Hybrid approaches combining positive control in dense zones with self-separation in lower density areas have also emerged [10]. Therefore, elements of these different paradigms could potentially be adapted for eVTOL traffic management within urban airspaces [11]. Nevertheless, unique challenges arise from constraints like vertiport configurations, corridors, buildings, and limited aircraft maneuverability that will likely necessitate developing innovative tailored solutions.

While aviation studies offer useful foundations, important insights on managing traffic flows can also be drawn from research on ground transportation in confined spaces like roads tunnels, bridges, and skybridges. Thus, queuing models have been applied to optimize tunnel traffic light timing based on vehicle densities. For instance, slot-based mechanisms have been developed for automated vehicle coordination on narrow bridges by using variable speed limits combined with ramp metering in order to achieve high throughput on congested skybridges [12].

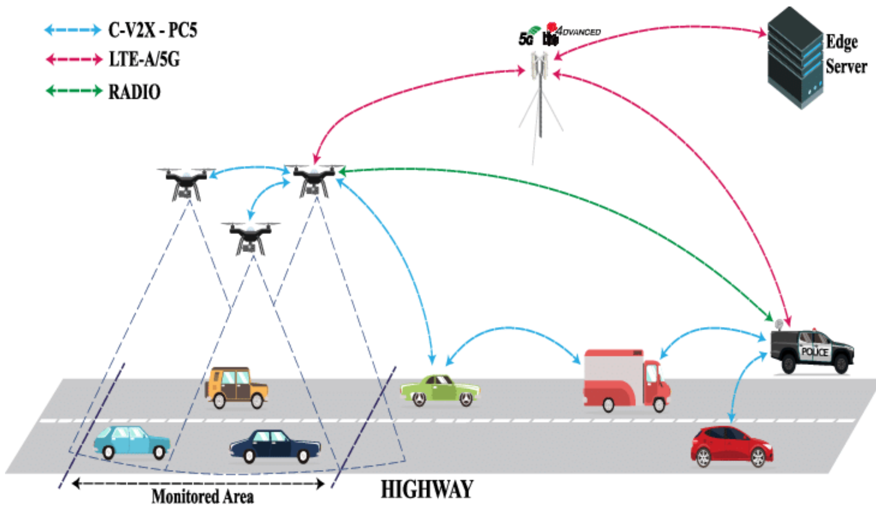

FIGURE 2.6 – Traffic flow in a confined space on a road. Photo from FLYEYE

However, adapting such concepts for eVTOL operations within narrow takeoff and landing corridors and precisely defined aerial routes above urban centres poses new complexities. Indeed, unique considerations like three-dimensional separation standards, aircraft performance constraints, and interactions between vertiport arrival and departure flows need to be addressed. This is why there is currently a study underway to explore the various possibilities for redesigning the airspace in order to make it usable by drones or eVTOLs, whether by fixing or not their degree of freedom so that they can move more easily and safely. Thus, some researchers are investigating the distribution of airspace into tubes or layers to better adapt to the expansion of large urban areas, all in order to reduce traffic congestion on roadways [13].

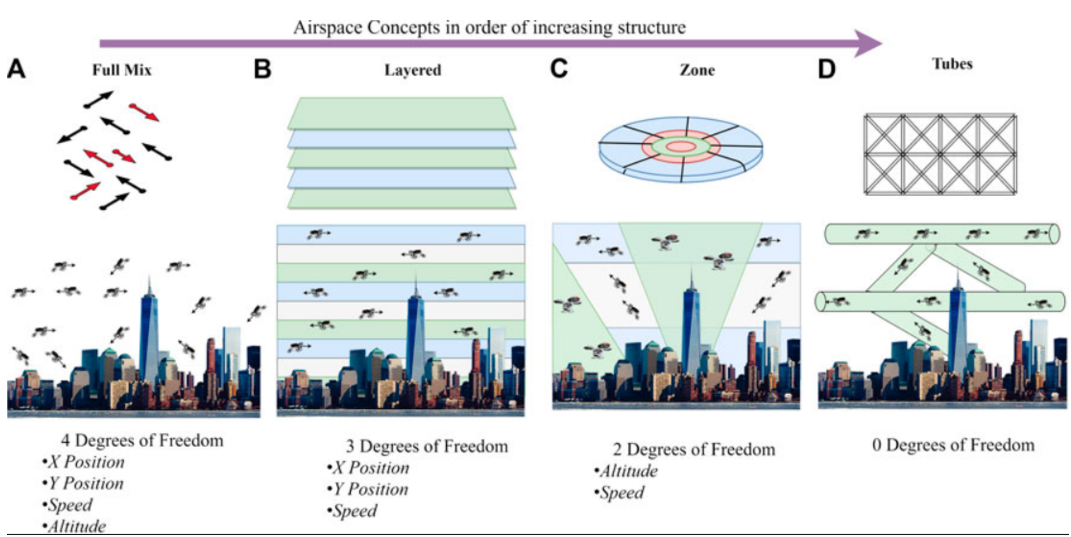

FIGURE 2.7 – Urban airspace concepts [13]

2.1.3 Managing traffic with eVTOLs

Thanks to significant technological advancements in recent years, drones have been utilized in various fields. Initially, they were used under human control, but gradually, efforts were made to make them autonomous in certain situations where they proved to be more efficient, resulting in significant time savings [14].

Many uses of drones are well-known, such as photography and delivery of goods, demonstrating their versatility and multiple utilities [15]. However, other lesser-known yet equally interesting examples have been developed recently and are under research, especially in the field of ecosystem maintenance. For instance, a drone model has been developed capable of deterring birds like a scarecrow so that they do not devastate farmers' crops in rural areas [16].

FIGURE 2.8 – Model of UAV developed by Wang to deter birds [16]

Similarly, another equally ambitious example is ensuring safety and rescue in urban areas by autonomous drones, which is a field that has been rarely explored until now. While many are familiar with civilian rescue operations in mountainous regions, for example, when helping people in extreme situations in the wilderness, civilian rescue in urban areas is a very recent field of study that requires thorough examination and the study of issues such as optimizing trajectories for these autonomous drones [17]. These very promising models, therefore, are worth exploring and will likely be means of addressing many issues in the future, across a wide range of fields.

2.2 Ensuring urban safety

This section will discuss how to ensure urban safety with rescue missions, focusing on the added value of eVTOLs compared to other aircraft, and will present some algorithms currently being studied by scientists to manage urban traffic for rescue operations.

2.2.1 Transition from helicopters and drones to eVTOLs

First of all, helicopters have long been indispensable assets in rescue operations, celebrated for their unparalleled capability to navigate through challenging terrain and swiftly transport rescue teams and essential supplies to remote or inaccessible locations. Their ability to access remote areas quickly, even in adverse weather conditions, underscores their crucial role in saving lives during emergencies. For example, UH-60 Black Hawk search and rescue helicopters have earned widespread acclaim for their versatility and reliability in responding to a diverse range of emergency scenarios, from natural disasters to mountainous terrain and maritime rescues. Consequently, their agility, coupled with the capacity to operate at low altitudes, renders them exceptionally adept at maneuvering through the intricate and unpredictable environments encountered during rescue missions [18].

FIGURE 2.9 – A Bell helicopter rescueing a victim in a mountain. Photo from HeliHub

In parallel with helicopters, drones have emerged also as invaluable assets in modern rescue operations, offering distinct advantages such as increased flexibility and portability. Unlike helicopters, drones can easily access confined or hazardous areas without risking the safety of crew members. Additionally, their compact size and maneuverability enable them to navigate through complex environments with ease. For example, DJI Matrice or Phantom drones have become indispensable tools for performing aerial reconnaissance missions in disaster areas [19][20]. Since they are equipped with advanced cameras and sensors, these drones provide real-time imagery to ground rescue teams, facilitating swift decision-making and coordination efforts during critical situations. Moreover, their ability to fly at high altitudes and cover large areas quickly makes them particularly useful for assessing damage and locating victims.

FIGURE 2.10 – Drone mapping a fire in a forest. Photo from Soliton Systems Europe leaflet

The transition from drones to eVTOLs marks a significant evolution in aerial transportation and rescue operations. Unlike drones, which are limited by their relatively short flight durations and payload capacities [18][19], eVTOLs offer enhanced capabilities that revolutionize the efficiency and scope of aerial missions. One key advantage of eVTOLs is their ability to carry heavier payloads over longer distances, making them ideal for transporting rescue personnel, medical supplies, and equipment to remote or inaccessible areas. This expanded payload capacity allows eVTOLs to address a wider range of emergency scenarios and provide more comprehensive support to rescue teams on the ground [21].

Moreover, eVTOLs boast greater speed and maneuverability compared to drones, enabling them to rapidly respond to emergency situations and reach affected areas within shorter timeframes. This increased speed not only accelerates the delivery of critical resources but also facilitates the timely evacuation of individuals in distress, minimizing response times and enhancing overall operational efficiency. Additionally, eVTOLs can operate at higher altitudes [22] and navigate through adverse weather conditions more effectively than drones, ensuring greater reliability and resilience in challenging environments.

Furthermore, the vertical take-off and landing capabilities of eVTOLs enable them to access confined or obstructed spaces with greater ease and precision than traditional aircraft. This flexibility allows eVTOLs to navigate through urban landscapes, dense forests, and mountainous terrain, providing unparalleled access to areas that are inaccessible to ground vehicles or helicopters. By leveraging their vertical flight capabilities, eVTOLs can execute complex rescue missions with precision and agility, reaching individuals in need of assistance with unparalleled speed and efficiency in a very demanding environment [23].

	eVTOLS	**Civilian drones**	**Helicopters**
Speed	100 to 400km/h	30 to 100km/h	100 to 250km/h
Range	0 to 1000kms	0 to 50kms	0 to 700kms
Payload Capacity	0 to 1000kgs	0 to 20kgs	0 to 1000kgs
Flight Endurance	30min to 4h	30min to 4h	30min to 4h
Altitude	0 to 5000m	0 to 500m	0 to 6000m

TABLE 2.1 – Table of average performance between aircrafs [14][15][18][19][20][21]

2.2.2 UAV/UAM traffic management research

Considering the findings in the previous section, which highlighted eVTOLs as the most promising aircraft type, it is pertinent to explore the research conducted on managing this traffic in urban environments. Nowadays, some recent studies exist on managing unmanned aerial vehicle (UAV) and urban air mobility (UAM) traffic. Indeed, studies have developed autonomous flight coordination algorithms using leader-follower arrangements, artificial potential fields, and swarming approaches to enable collision-free operation of drone fleets. For instance, there are huge international agencies like the following presented on the figure 2.11, which are developing such models of VTOLs, trying to reconcile these various issues.

In parallel with this, NASA's Advanced Air Mobility (AAM) research aims to revolutionize our communities by shifting the transportation of people and goods from ground-based to on-demand, airborne solutions. This future air transportation system will encompass low-altitude passenger transport, cargo delivery, and public service functionalities [24].

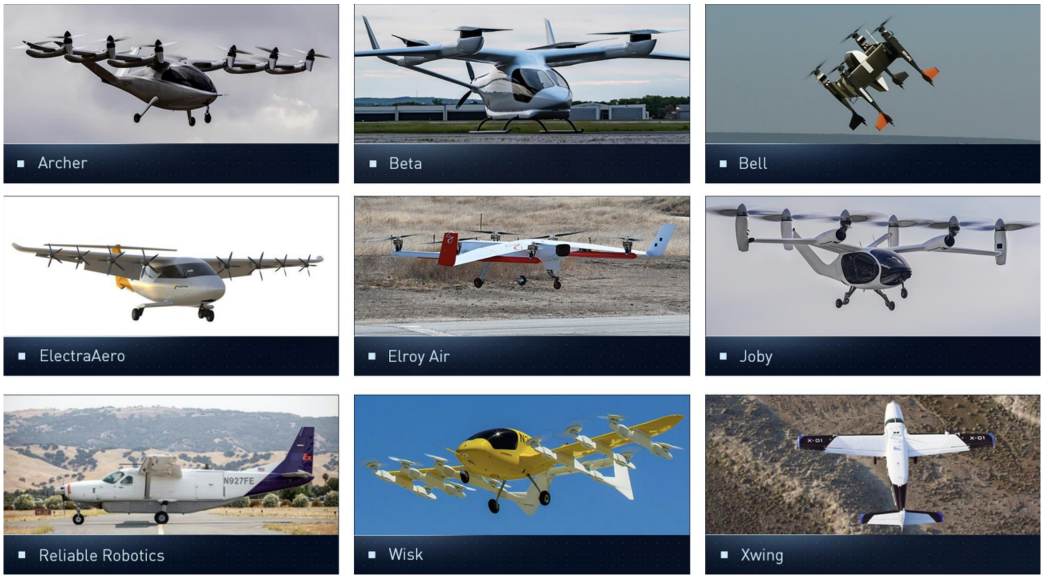

FIGURE 2.11 – Different models developed by agencies [24]

Besides, decentralized model predictive control and distributed receding horizon control have been applied for cooperative path planning among UAVs. In addition, machine learning techniques like reinforcement learning show promise for optimizing dynamic routing and scheduling. For instance, collision avoidance systems based on ADS-B-like data exchange, sensor arrays, and detect-and-avoid algorithms have also been tested for UAVs. Similarly, trajectory planning optimization leveraging mixed-integer linear programming, genetic algorithms, and ant colony optimization has been used to generate efficient UAV routes meeting operational constraints [25]. Regarding the segregation of zones and rules for priority access, airspace management models have been proposed using concepts like dynamic geo-fencing.

However, most of this research has focused on UAV coordination in wide areas or at low densities, rather than congested urban environments and higher-throughput eVTOL vertiport operations. Indeed, some key considerations like the effects of vertiport layouts, limitations of aircraft maneuvering, higher traffic densities, and contingency procedures have received limited attention so far.

2.2.3 Types of planning for the mission

As noted in the preceding section, various aircraft are available for conducting search and rescue missions. Therefore, this section will deals with the different ways to optimize the path to realize search and rescue missions to save people in extreme situations.

Actually, finding an algorithm which would be able to gather all the criteria to be used in all missions do not exist. That is the reason why trajectory planning algorithms for drones are systematically categorized to align with specific mission requirements, employing an approach that emphasizes functional characteristics. This classification is grounded in three distinct perspectives : time-based planning, space-based planning, and mission-based planning. Each perspective evaluates how algorithms address unique mission considerations.

Firstly, time-based planning involves the analysis and categorization of algorithms based on their temporal characteristics, assessing their capacity to navigate the time constraints inherent in drone missions. This perspective takes into account the responsiveness and adaptability of algorithms to dynamic and time-sensitive environments [26].

Secondly, space-based planning hones in on the spatial aspects of trajectory planning algorithms, evaluating their effectiveness in handling the spatial complexities of the environment, encompassing obstacles, terrain, and three-dimensional space. Algorithms are categorized based on their proficiency in managing these spatial features [27].

Lastly, mission-based planning classifies algorithms according to their alignment with specific mission requirements. Various drone missions may necessitate distinct trajectory planning approaches, such as area coverage, target visiting order, or mission parameter optimization. This perspective scrutinizes how algorithms meet the specific objectives of each mission [28].

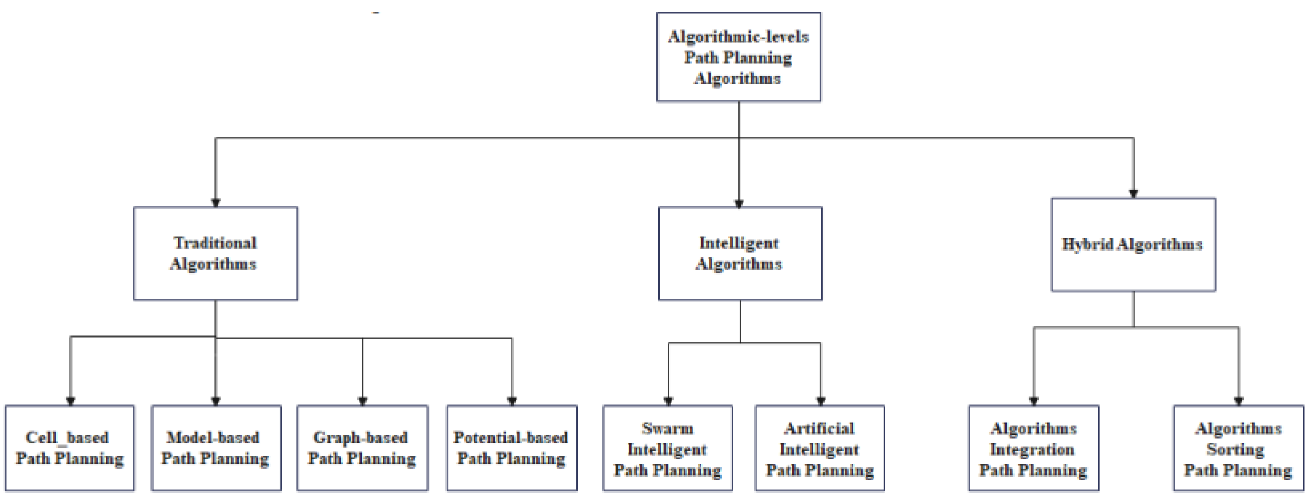

FIGURE 2.12 – Classification of algorithm-level UAV path planning. Photo from MDPI

Therefore, it is crucial within a mission to break down the seemingly insurmountable major problem into a multitude of minor problems. Each algorithm can then leverage its specific strengths so that once all these minor problems are resolved, the major problem is addressed comprehensively.

2.2.4 Main algorithms existing

In the present day, there are already existing algorithms which present strong advantages. For instance the reinforcement learning algorithms for drone trajectory planning include their ability to learn through interaction with the environment, optimize decisions, and provide solutions tailored to continuous state or action spaces.

Moreover, these algorithms can be combined with deep learning techniques to address the evolving needs of the airspace. However, disadvantages encompass the discrete nature of state and action spaces, potentially making the planned trajectory challenging to navigate and manage dynamic threats. Additionally, reinforcement learning algorithms may encounter convergence issues and require suitable datasets for training.

Therefore, scientists have been able to develop different categories of space-based drone trajectory planning algorithms which are the following :

— Cell-based algorithms : utilize a synthesis of graphical and mathematical methodologies for trajectory planning, including algorithms such as A* and its variants [29].
— Mathematical model-based algorithms : rely on a diverse set of mathematical models, including planning models and probabilistic models, as well as mathematical equations and functions such as Lyapunov functions [30], Bessel curves [31], and Dubins curves [32].
— Node-based algorithms : focus on scaling nodes and include innovative orientation-based search strategies, directional search strategies, adaptive step strategies, adaptive weight strategies, bidirectional search strategies, and a reallocation process within the A* framework [33][34].
— Sampling-based algorithms : employ sampling techniques to generate potential trajectories and assess their feasibility [35].

2.3 Gap analysis

Therefore, the literature review has shown a world experiencing rapid demographic expansion, particularly in large urban areas, and multiplying threats due to medical, climatic and demographic reasons. Consequently, a quick and effective reaction at any moment is necessary.

One solution currently under study involves eVTOLs, which are autonomous electric drones that offer characteristics and potential even more interesting than drones and helicopters in an urban environment. Given the current limited or nearly nonexistent research, the focus of the remainder of the thesis will be the study of managing trajectories of such eVTOLs in an urban environment where they could interact between them for teams missions [36] by simulating obstacles with different algorithms to create a credible, reliable model to use in the near future.

3 Methodology

This section details the elements of the strategy implemented to address the issue. It involves building a naive and credible model capable of addressing all possible situations, then comparing it with a more optimized model before complicating the scenario and applying it to a concrete situation. Thereafter, all non-referenced images will be screen captures taken with Matlab software.

3.1 Framework

The methodology follows these steps :

1. Create a credible two-dimensional environment to test various algorithms.
2. Establish a credible scenario for urban rescue.
3. Test a naive algorithm capable of detecting and avoiding multiple static obstacles, non-optimized but effective.
4. Test an optimized algorithm in the same environment and scenario to compare the models.
5. Complexify the scenario with multiple eVTOLs.
6. Apply the two algorithms to a concrete case study.

3.2 2D environment model

The environment used is two-dimensional and has been simplified as a square with a side length of two kilometres, as shown in figure 3.1. Several characteristic points and zones have been defined in the legend to figure 3.1. Others that are not detailed in the legend are listed below :

— a quadricopter representing the eVTOL.

— a sensor range to detect obstacles (blue).

— a target to save (a black cross).

— obstacles which are not represented here (circle).

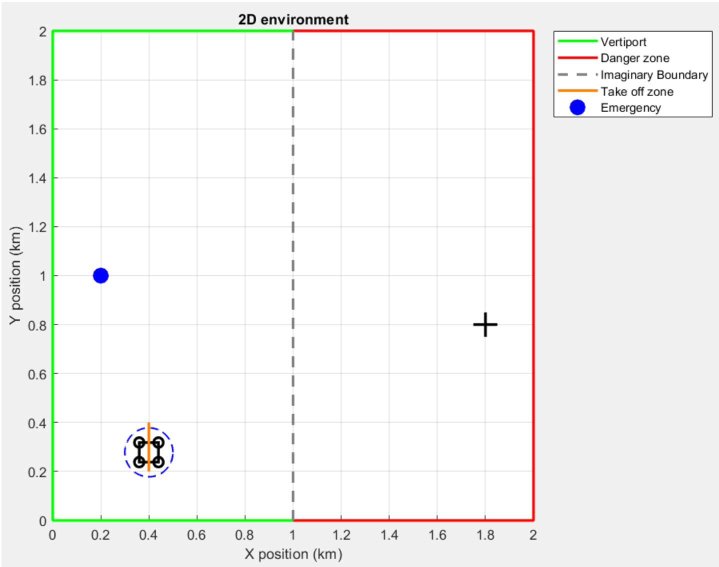

FIGURE 3.1 – Environment model

3.3 Study hypotheses

3.3.1 eVTOL model

The eVTOL is named Vertiia and is developed by the company AMSL Aero which currently works with the Bankstown Airport in Sydney, possessing the following performances :

— 1000km range
— 300km/h speed
— 500kg payload
— operating costs up to 70% lower than a helicopter

FIGURE 3.2 – Vertiia eVTOL model [24]

3.3.2 Simulation hypotheses

To ensure the simulations are as rigorous as possible, the following experimental conditions were established :

— the takeoff point position is fixed.

— the position of the target to be rescued is fixed.

— the position of the point where to bring back the target is fixed.

— the positions of the obstacles are placed randomly but coherently to require the eVTOL to dodge them.

— the eVTOL is not aware of the obstacles' locations ; its detection radius will guide it progressively during its progress (only for the naive algorithm).

3.4 Naive algorithm

This sub-section gives the general ideas of the algorithm. The algorithm itself can be found in the GitHub link in the appendices, where the various functions used are detailed in the README. This algorithm has been built from scratch and has not been inspired by any previous project.

3.4.1 Logical diagram

The philosophy of the naive algorithm can be represented in the form of a logical diagram, with the primary objective of enabling any eVTOL in any arrangement to successfully complete its mission. If the position and number of obstacles make the mission too challenging, an emergency protocol is initiated for the eVTOL to resume a random position.

This algorithm is not very optimised, particularly when too many obstacles are present. The guiding principle is that the eVTOL should be autonomous enough to reach the target to be rescued and bring it back to the emergency point, namely the "end point" on figure 3.3.

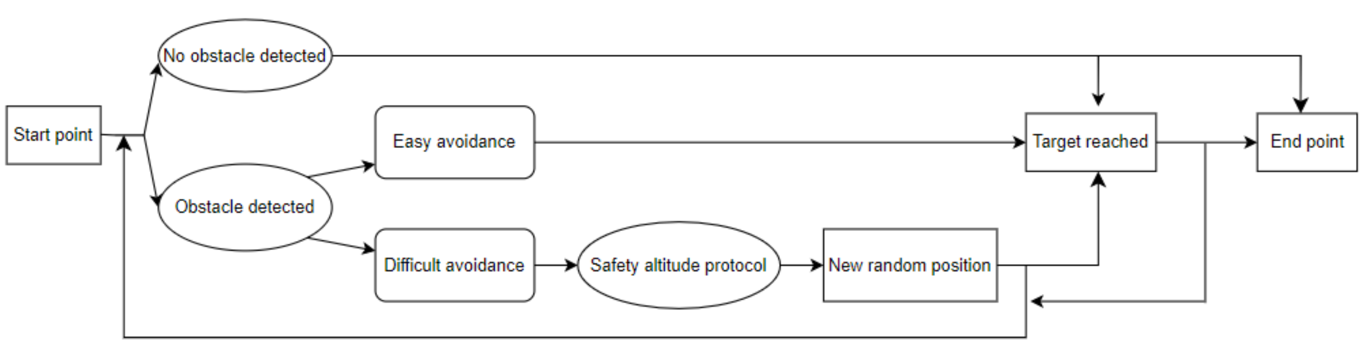

FIGURE 3.3 – Block diagram for naive algorithm

3.4.2 Operation of obstacle detection

The main idea for the obstacle avoidance is that a sensor range has been placed all around the quadcopter's square, and with each iteration and advancement of the eVTOL, the detectors act with a certain radius to see if an obstacle enters their field or not. Thus, this algorithm acts as if each detector therefore scans a 90° zone. Specifically, the division has been made into four zones : northeast, northwest, southeast, southwest.

On figure 3.4, the northeast part of the sensor will detect the obstacle, before trying to avoid it.

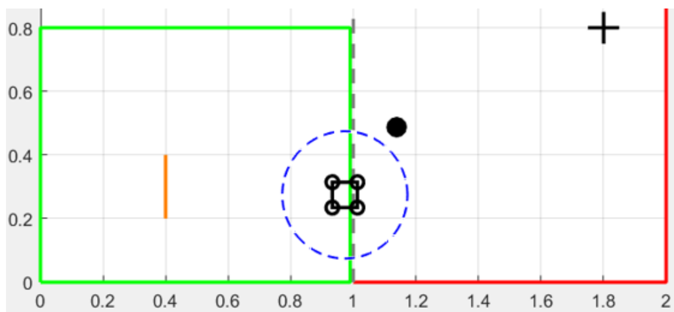

FIGURE 3.4 – Sensor range of the eVTOL close to an obstacle

Algorithm 1 below provides a simplified description of how the eVTOL detects an obstacle using its detection radius. In other words, as soon as the distance between the detection radius and the obstacle is less than the detection radius, one part of the sensor range (south-east, south-west, north-east, north-west) will detect an obstacle and start a counter which will then be used for obstacle avoidance.

Algorithm 1 Naive algorithm : obstacle detection

```
INITIALIZATION :
Initialize : environment, handles, eVTOL parameters, threshold, ObstaclePosition, the initial position of the eVTOL, x_temp and y_temp
while distance between eVTOL and target is greater than threshold do
    Calculate trajectory between eVTOL and target for x and for y
    Increment x_temp by the difference between x_temp and the next calculated ideal trajectory position for x
    Increment y_temp by the difference between y_temp and the next calculated ideal trajectory position for y
    Refresh obstacle sensor state by calling sensorDetectionForObstacle
    while the smallest distance between any eVTOL sensor and the obstacle is less than detection radius and the obstacle is between the target and eVTOL do
        if the sensor that detected the obstacle is the same as the previous one then
            Increment cpt by 1
        end if
    end while
end while
```

3.4.3 Operation of obstacle avoidance

Regarding obstacle avoidance, it is based on a basic principle. If the eVTOL detects an obstacle with one of its four sensors, it will redirect itself in the opposite direction.

It is important to note, however, that there are two cases to consider. The first is the case of easy avoidance ; easy because the eVTOL is not aligned in the same axis as the obstacle and the target. In this case, avoidance is easily achieved by moving away from where the obstacle was detected, and thus the avoidance occurs gradually.

For instance on figure 3.5, the eVTOL has detected the obstacle from the northeast side. Therefore, it will move on the opposite side with a unit movement chosen accurately in order to have a smooth path, coherent with what could happen in a real life. This is the repetition of such movements that progressively avoids the obstacle.

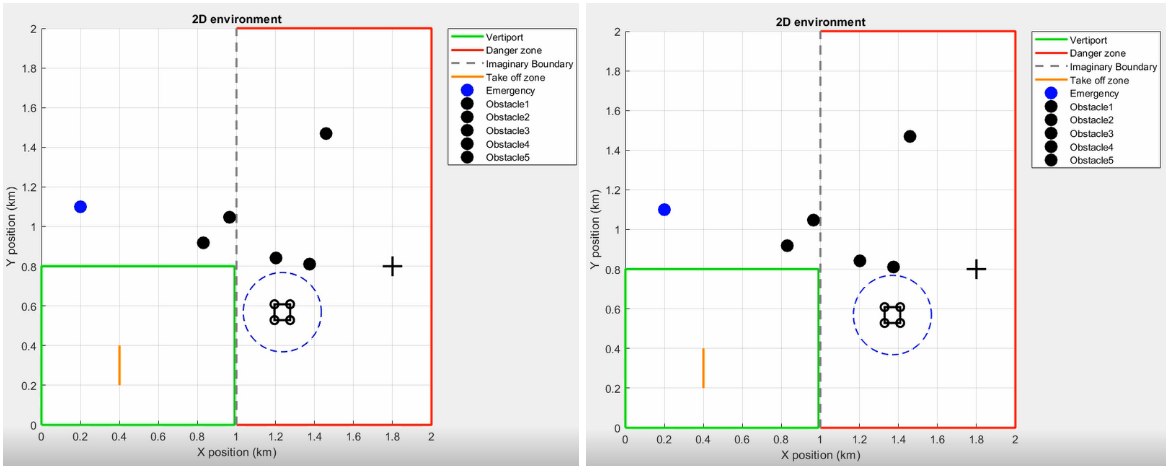

FIGURE 3.5 – Avoidance from a northeast obstacle

Likewise, on figure 3.6, the obstacle is placed on the southwest side, therefore it will avoid the obstacle by moving back on the northeast before avoiding it completely and going straight to the target.

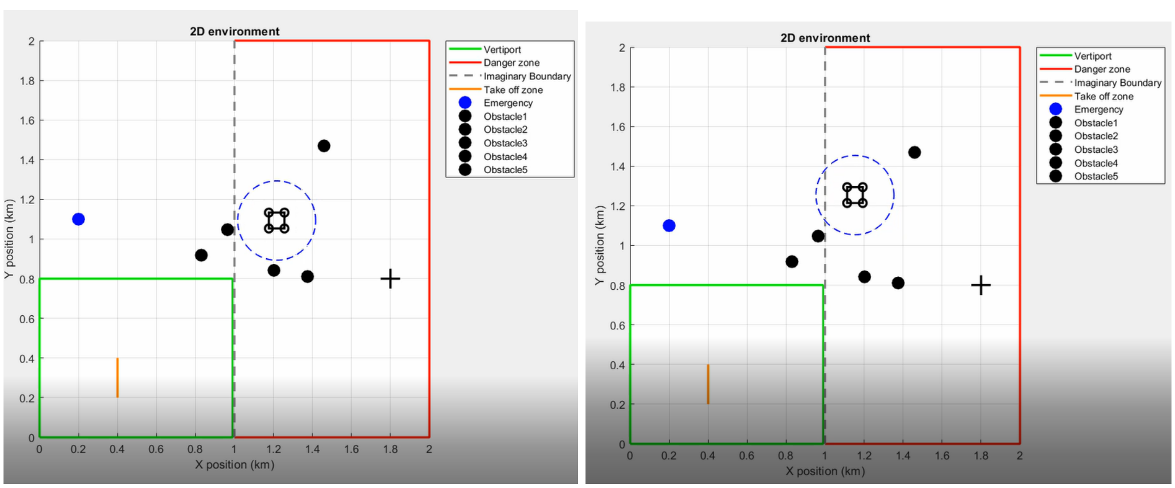

FIGURE 3.6 – Avoidance from a southwest obstacle

In the case where the obstacle is on the perfect straight line between the eVTOL's point of departure and the target, it is problematic to avoid the obstacle. Avoidance is based on detection by one of the four sensors located on the eVTOL's rotors, but if the eVTOL detects an obstacle before its north-east sensor, it is instructed to go in the opposite direction, south-west. However, if the target is to the north-east, it will return to the place where it was blocked because its sensor will detect the obstacle again. The result is a succession of back-and-forth movements.

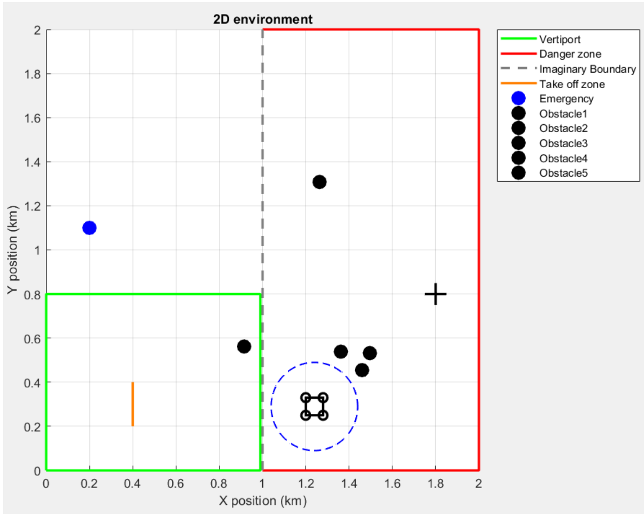

FIGURE 3.7 – Contentious case when an eVTOL and a target in a straight line

The solution chosen here was to stipulate that once this succession of back-and-forth movements, symbolised by a counter, exceeds a certain threshold, the eVTOL will reach a safety altitude because it understands that the situation is not conventional and not trivial. By doing this, it would surpass the obstacle in altitude, which is a situation that would be close to the reality.

In addition, once this safety altitude has been reached, it is instructed to take a random position around itself (excluding that of the obstacle or target), in order to repeat the process until the success of the mission. For instance, in figure 3.8 on the left, a scenario depicts an eVTOL encountering an obstruction. Consequently, upon reaching a certain threshold, it chooses a new random position to restart the process like describes in algorithm 2 below.

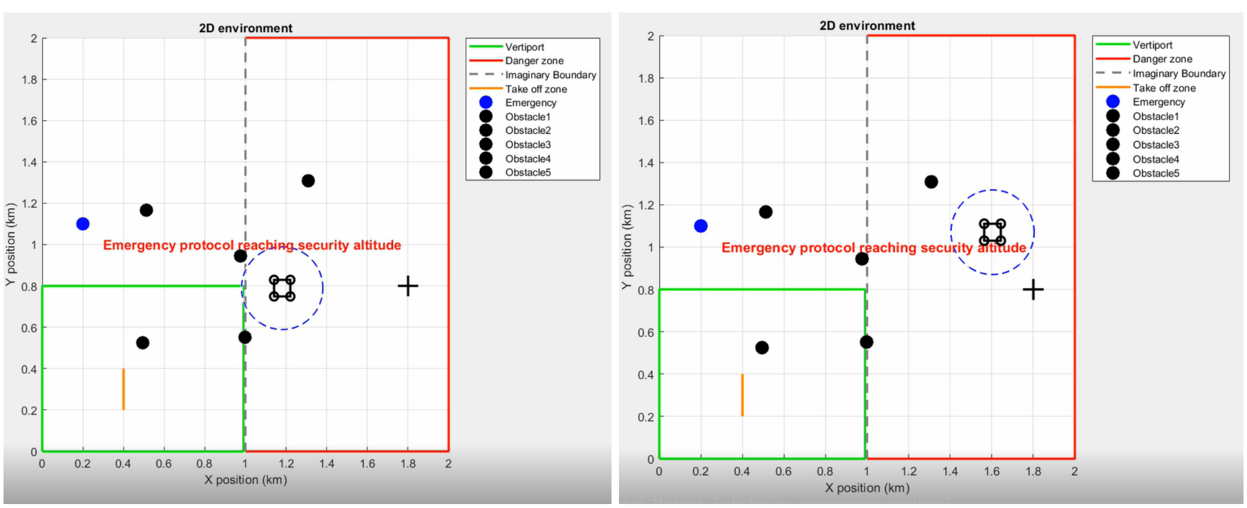

FIGURE 3.8 – Emergency protocol

Algorithm 2 Naive algorithm : obstacle avoidance

```
INITIALIZATION :
Initialize : environment, handles, eVTOL parameters, threshold, ObstaclePosition, the initial position of the eVTOL, x_temp and y_temp
while distance between eVTOL and target is greater than threshold do
    x_temp = x_temp + the difference between x_temp and the next ideal x
    y_temp = y_temp + the difference between y_temp and the next ideal y
    Refresh obstacle sensor state by calling sensorDetectionForObstacle
    while the smallest distance between any eVTOL sensor and the obstacle is less than detection radius and the obstacle is between the target and eVTOL do
        if the sensor that detected the obstacle is the same as the previous one then
            Increment cpt by 1
        end if
        if cpt equals 50 then
            Generate a random waypoint
            while distance between the waypoint and eVTOL is greater than threshold do
                x_temp = x_temp + the difference between x_temp and the next ideal x
                y_temp = y_temp + the difference between y_temp and the next ideal y
                Update handles displaying eVTOL on the graph with deletall
                Display emergency protocol message
            end while
            Reset cpt to 0
        end if
        SWITCH id_min (sensor index that detected the obstacle)
        CASE 1 :
        Increment X_temp and y_temp by 0.1
        Update handles, eVTOL position and previous_id_min
        BREAK
        CASE 2 :
        Increment X_temp by 0.1
        Decrement y_temp by 0.1
        Update handles, eVTOL position and previous_id_min
        BREAK
        CASE 3 :
        Decrement X_temp by 0.1
        Increment y_temp by 0.1
        Update handles, eVTOL position and previous_id_min
        BREAK
        OTHERWISE :
        Decrement X_temp and y_temp by 0.1
        Update handles, eVTOL position and previous_id_min
        BREAK
    end while
    Update handles displaying eVTOL on the graph
end while
```

3.5 A* algorithm : an optimized path

Unlike the naive algorithm, the A* algorithm is inspired by work already carried out by developers and has been adapted to come as close as possible to the experimental conditions of the naive algorithm. This algorithm is also detailed in the GitHub link where the various functions are explained.

Furthermore, the A* algorithm does not generate a real-time simulation, but takes a screenshot of the path taken by the eVTOL to pick up the target before returning it to the emergency point. In fact, in order to calculate the mission completion time, it was necessary to set a parameter for the eVTOL, in this case its speed. The speed was set so that the unobstructed mission would have the same average time. In fact, with no obstacles, both are supposed to have the same travel time, whatever the algorithm, since the trajectories will be straight sections.

For instance, figure 3.9 shows two simulations with obstacles (big black circles), and straight lines drawn between the starting point (takeoff zone), the target (black cross) and the emergency point (blue circle). On the way to the target, the eVTOL follows a perfectly straight trajectory, and on the way back, the A* algorithm calculates the most optimised path by considering each new node, or new possible neighbour, taking care not to hit the obstacle and to reach the emergency point.

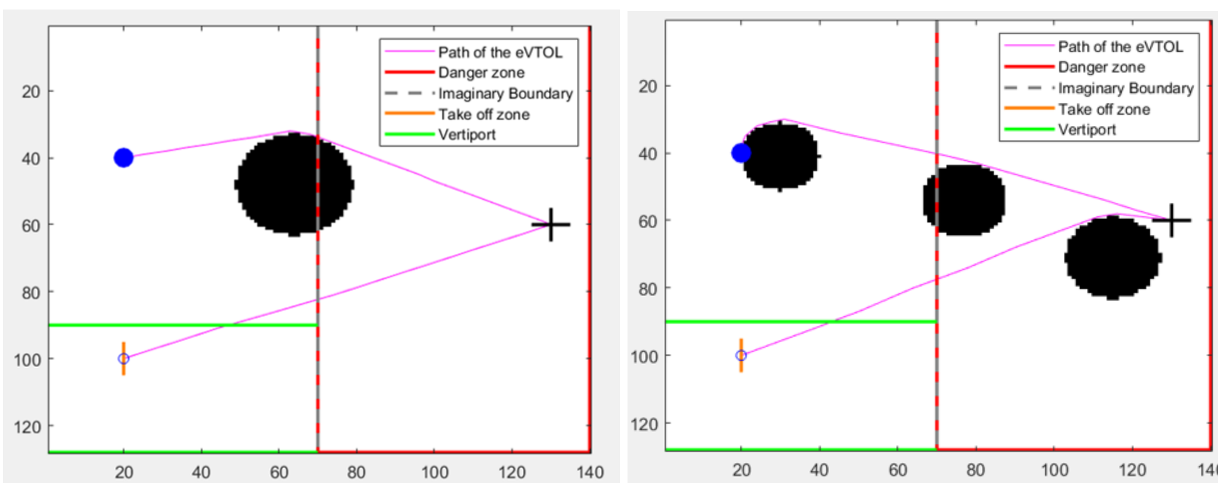

FIGURE 3.9 – eVTOL path optimised with A* algorithm

In this example, the principle is the same, even if the trajectories sometimes appear to be curved. In reality, they are not curved; they are just very small portions of straight lines that can only be seen when zoomed in.

Since the naive algorithm simply achieves the desired result without optimising the path, the A* algorithm produces a much more interesting path. The guiding principle is the generation of a large number of points between the start and end points and connects them with small straight lines.

The system as a whole will then be servo-controlled using different correctors to find out which one would best correct this succession of straight lines at the points generated. The algorithm 3 describes concisely how the A* works.

Algorithm 3 A* algorithm

Input : Take off point, Target point, Emergency point, Obstacle map
Output : Travel time of eVTOL from Take off to Emergency point via Target point with obstacle avoidance
INITIALIZE open set with take off point
INITIALIZE closed set as empty
INITIALIZE found target as false
INITIALIZE travel time as 0
while open set is not empty and found target is false **do**
    Select node with lowest f-value in open set (f = g + h)
    if selected node is target point **then**
        Set found target as true
    else
        if selected node is emergency point **then**
            return Travel time
        end if
        Move selected node from open set to closed set
        for each neighbor of selected node **do**
            if neighbor is not in closed set and neighbor is not an obstacle **then**
                Calculate tentative g-value for neighbor
                if neighbor is not in open set or tentative g-value is lower **then**
                    Update neighbor's parent and g-value
                    Calculate heuristic h-value for neighbor
                    Calculate f-value for neighbor (f = g + h)
                    Add neighbor to open set
                end if
            end if
        end for
    end if
    Increment travel time
end while
return Travel time if target reached or no valid path found

3.6 Test of Shapiro-Wilk

It is not so straightforward to compare the naive algorithm and the A* algorithm. Indeed, although the MATLAB codes used had the same simulation conditions, they did not generate the same coordinates for the positioning of obstacles during the hundreds of simulations conducted. Consequently, it would only be coherent to consider a comparison if and only if the two distributions follow the same statistical law. By conducting hundreds of simulations, a visual trend emerges, that of a normal distribution with a Gaussian curve. Therefore, it is appropriate to perform statistical tests to verify whether or not the distributions allow for a coherent comparison.

For this, a Shapiro-Wilk test will be tested to check whether the distributions follow a normal distribution or not. There are two hypotheses :

— H_0 : the distribution follows a normal distribution

— H_1 : the distribution does not follow a normal distribution

The Shapiro-Wilk test statistic is given by :

$$W = \frac{\left(\sum_{i=1}^{n} a_i x_{(i)}\right)^2}{\sum_{i=1}^{n}(x_i - \bar{x})^2}$$

where :

— $x_{(i)}$ represents the i-th order statistic (the i-th smallest value in the sample)

— $\bar{x}$ is the mean of the x_i

— a_i are constants that depend on the sample size n

From the statistic W, it can be determined the p-value from a table, which should be compared to α, the desired significance level. If the p-value is less than the significance level α, it means that H_0 is rejected, and the distribution does not follow a normal distribution.

If the p-value is greater than the significance level α, it means that H_1 is rejected, and the distribution follows a normal distribution.

In that case, this table which summarizes the possible results will be followed, considering the significance level with an α equals to 0,05 :

Table 3.1 is derived from mathematical results found and compiled on the Internet. As of today, there are no precise values to determine categorically whether or not values perfectly follow a normal distribution. Experimental conditions indeed have a significant influence, especially when many parameters are involved, which is the case here. Therefore, it is appropriate to be quite flexible and broad in the intervals chosen in this table, as well as in their interpretation.

P-value	**Probability of following a normal distribution**
> 0.10	Very high
0.10 - 0.05	Moderately high
0.05 - 0.01	Medium
0.01 - 0.001	Low
< 0.001	Very low

TABLE 3.1 – Correspondence between p-value and probability of following a normal distribution

A Python program included in the appendices (figure 8.1) returns the value of the W statistic, the p-value, and its corresponding probability of following a normal distribution by simply replacing the data column with the column to be considered, which is also found in the Excel files in the appendices.

3.7 Complexification of the scenario : multiple eVTOLs

In the algorithms described previously, only one eVTOL is considered to rescue a single target. In reality, it may be necessary to rescue multiple targets simultaneously.

Furthermore, up until now, both the naive and A* algorithms considered only static obstacles, which could represent humans, road signs, inaccessible zones, or turbulence areas. However, in everyday life, it is common to interact with dynamic external factors. This is why, when multiple eVTOLs are deployed on a mission together to rescue multiple targets, one eVTOL will consider the other eVTOLs as dynamic obstacles, acting as a priority system during their movements.

For the future, the flight and priority rules are not the same as the simulation hypotheses in 3.3.2 but are defined as follows and in the figure 3.10 :

- eVTOLs will depart from the same starting point (take off zone).
- eVTOLs will rescue different targets (blue or red crosses).
- eVTOLs will head to different hospitals (blue or red emergency point).
- on the outward path, the first eVTOL to move will be the one furthest from its target.
- on the return path, priority will be given to the eVTOL closest to its respective hospital.

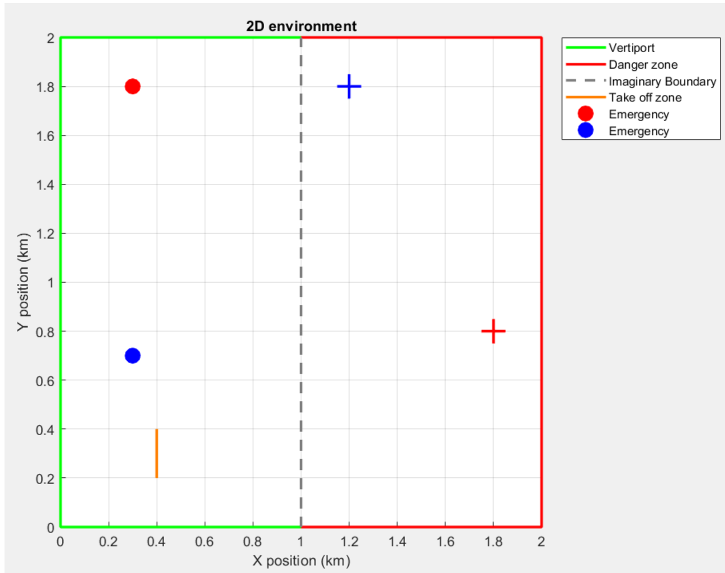

FIGURE 3.10 – Environment for multiple eVTOLs

3.8 Application to a concrete scenario

As the two algorithms provide a high success rate, it is appropriate to apply them to a recent concrete case study.

On April 13, 2024, a tragic stabbing attack occurred at the Westfield shopping center in Bondi Junction, Sydney. Joel Cauchi, a 40-year-old man with a history of mental health issues, carried out the attack where he stabbed multiple people, resulting in six fatalities, including a student from the University of Sydney.

For this experiment, the freely accessible NSW Planning Portal Spatial Viewer website was used to access topographic and specific data for the city of Sydney, including the height of buildings.

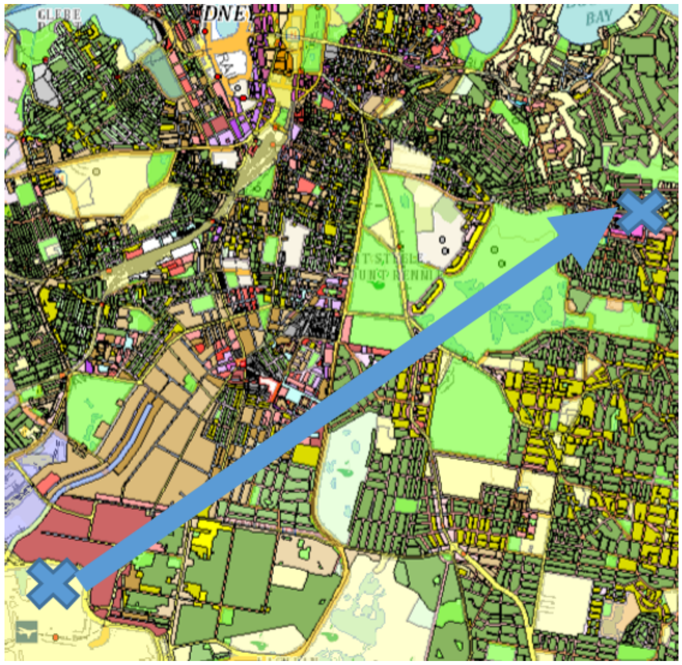

FIGURE 3.11 – Map of Sydney

In figure 3.11, the starting point is indicated as Sydney International Airport, and the end-point as the Bondi Junction shopping center. The nearest hospital to the shopping center is located a few hundred meters away. Therefore, the route from the shopping center to the hospital will not be considered. For the next part, the cruising altitude will be considered as the minimum altitude currently allowed for drones in Sydney, which is 400 feet, or approximately 130 meters. Consequently, along the route connecting the airport and the shopping center, the following will be considered obstacles :

- a cluster of buildings, regardless of their height.
- isolated buildings with an altitude exceeding 130 meters.
- restricted areas such as parks and prisons etc.

Figure 3.12 provides a detailed view of the different areas along the route from the airport to the shopping center, including the various building heights, clusters of buildings, and restricted access zones.

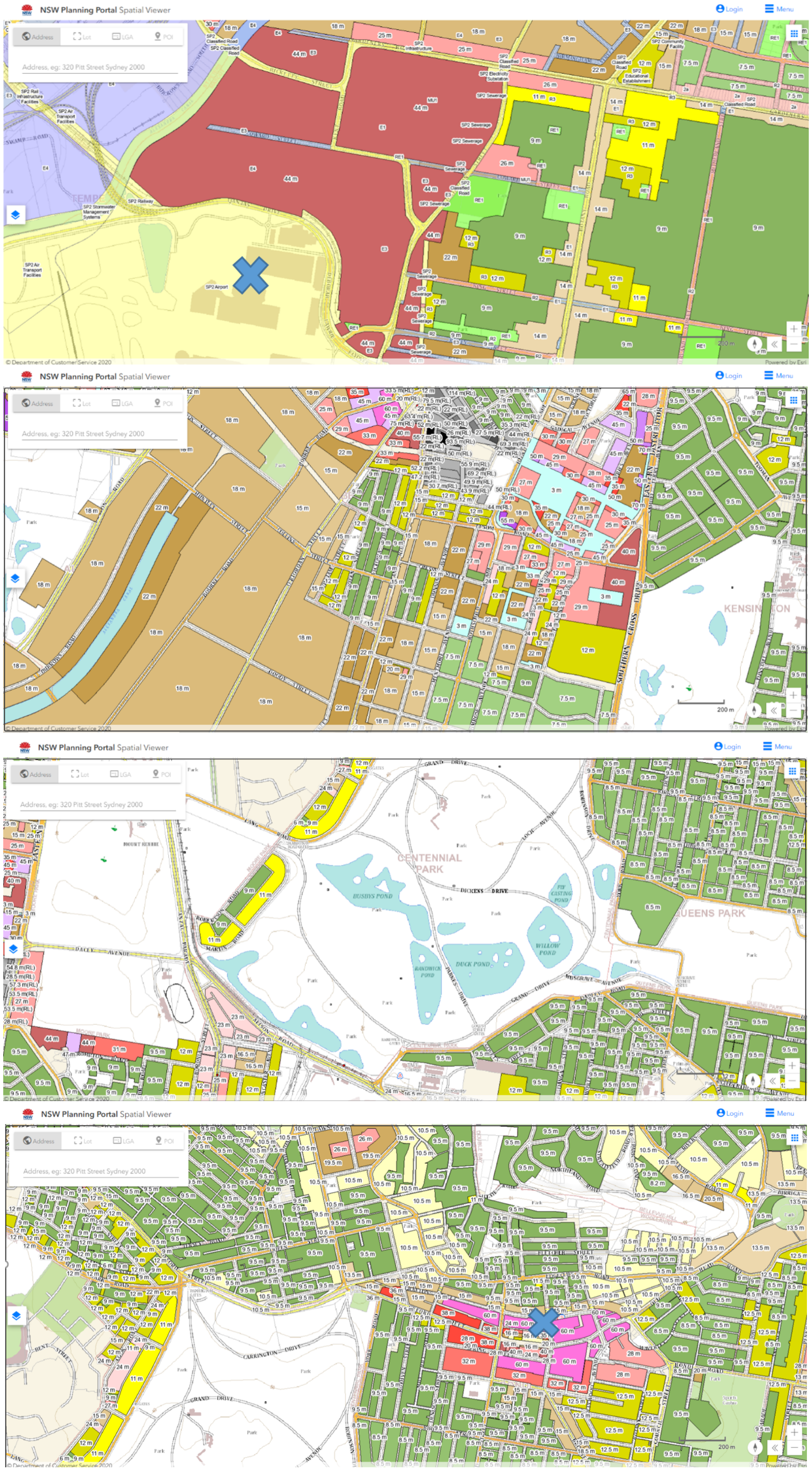

FIGURE 3.12 – Detailed map with the height of buildings and specifities

4 Results

This section contains all the results obtained from the various simulations carried out using the different algorithms and tests described throughout this thesis. All the simulations carried out in Matlab have been recorded in an Excel file which can be found in the appendices.

4.1 Shapiro-Wilk test

The Shapiro-Wilk test was applied to obtain the W statistics and the corresponding p-value for the naive algorithm considering the different cases with varying numbers of obstacles. The p-value, varies between 0,032 and 0,119, which means in other terms according to the Shapiro-Wilk test that the probability of following a normal distribution is between a high probability and a medium one, such as presented in the table 4.1.

	W statistic	**P-value**	**Probability of following a normal distribution**
0 obstacle	0,9887	0,119	High
1 obstacle	0,987	0,079	Moderately high
2 obstacles	0,9865	0,054	Moderately high
3 obstacles	0,9854	0,041	Medium
4 obstacles	0,982	0,037	Medium
5 obstacles	0,984	0,032	Medium

TABLE 4.1 – Shapiro-Wilk test for the naive algorithm

To draw a parallel between them, the Shapiro-Wilk test was also applied to the A* algorithm, also varying the number of obstacles. Here, the p-value varies between 0,09 and 0,141, which means according to the Shapiro-Wilk that the probability of following a normal distribution is high.

	W statistic	**P-value**	**Probability of following a normal distribution**
0 obstacle	0,9887	0,119	High
1 obstacle	0,9892	0,141	High
2 obstacles	0,9875	0,09	Moderately high
3 obstacles	0,9883	0,11	High
4 obstacles	0,981	0,099	Moderately high
5 obstacles	0,989	0,129	High

TABLE 4.2 – Shapiro-Wilk test for the A* algorithm

Comparing the values in the two tables, it can be observed that the overall p-value is higher for the naive algorithm, particularly as the number of obstacles increases. The reason why the p-value is greater for the naive algorithm than for A* lies in the fact that the more obstacles there are, the greater the probability that their disposal will require an emergency procedure to be triggered. Consequently, the emergency procedure lengthens the path time and widens the range of values obtained, thereby reducing the probability of following a normal distribution.

In conclusion, the Shapiro-Wilk test proves that in general the thousands simulations made are likely to follow a normal distribution especially when there are few obstacles. Thus, this is a interesting result that enable to draw gaussian curves for the two algorithms following a normal distribution according the Shapiro-Wilk test.

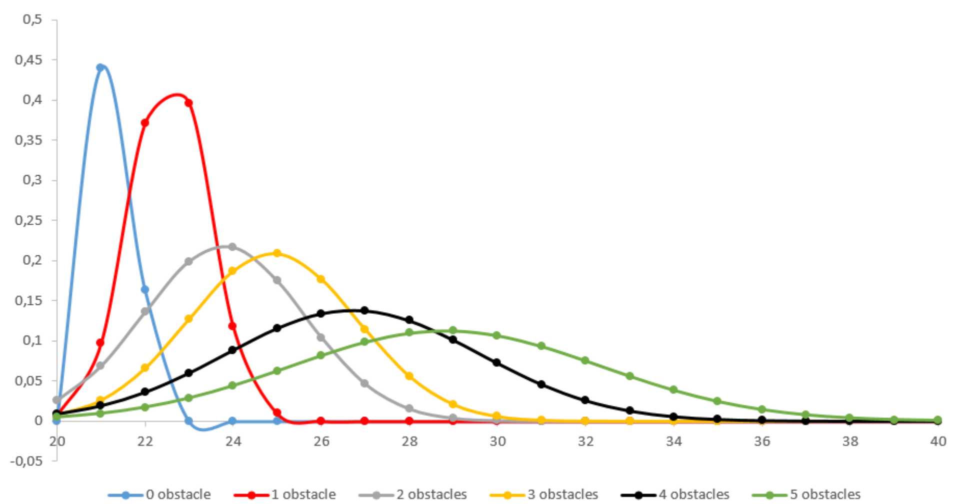

FIGURE 4.1 – Naive algorithm : normal distribution as a function of obstacles

Figure 4.1 shows that the Gauss curves collapse as the number of obstacles increases, which corroborates the remark made about table 4.1. This is why the reliability of the Shapiro-Wilk test weakens in accordance with the results in the table, since the curves are so crushed that they almost no longer follow a normal distribution.

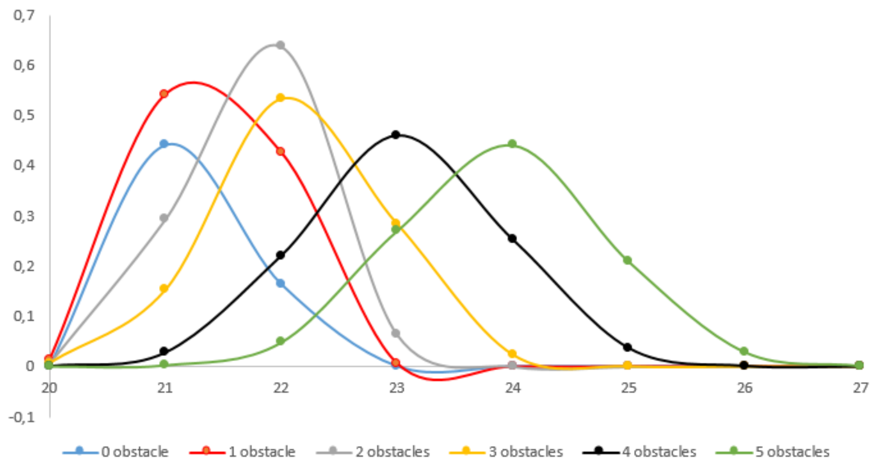

FIGURE 4.2 – A* algorithm : normal distribution as a function of obstacles

Conversely, figure 4.2 shows that the Gauss curves have the same shape, which also confirms that the Shapiro-Wilk test is more effective in confirming the hypothesis that the distribution follows a normal distribution with a high probability, as table 4.2 suggests.

4.2 Accurate sensor range

In order to make consistent measurements and to be able to compare the naive algorithm with a more powerful algorithm, the A* algorithm, an important parameter needs to be set for the remainder of the work, namely the detection radius. The smaller the detection radius, the later the eVTOL will detect the obstacle and the greater the risk of collision. Conversely, if the radius is too large, the algorithm will cause the eVTOL to take a trajectory that is too unlikely to be considered relevant. Hundreds of simulations have been carried out for detection radii ranging from 0.1 to 0.5 kilometres. The number of emergency protocols and the mission success rate were recorded.

Sensor range (km)	**Average time (s)**	**Average success (%)**	**Emergency protocol (%)**
0,1	23,59	100	0
0,2	28,82	99,5	9
0,3	34,95	92	23
0,4	41,91	77	54
0,5	51,68	51	82

TABLE 4.3 – Time, success and emergency protocol according to the sensor range

The results show that the success rate decreases the larger the detection radius. This is why, for the rest of the results, it was decided to opt for a detection radius of 0.2km, a choice that seems consistent with its success rate, average path time and the number of emergency procedures triggered. Possible problems include an unintended collision or the eVTOL getting stuck between several obstacles and being unable to move, as shown on figure 4.3.

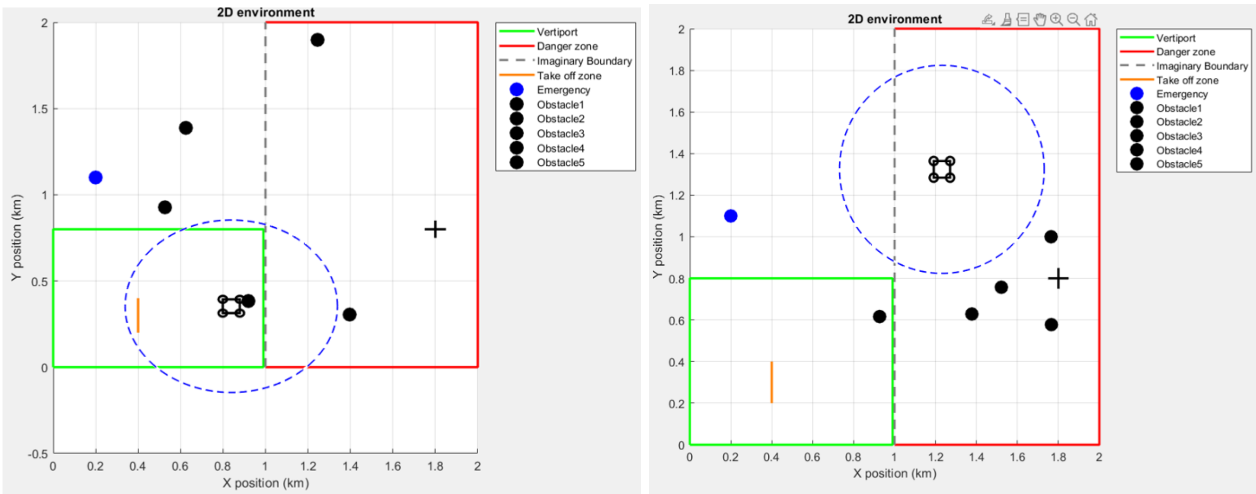

FIGURE 4.3 – Collision and arrangement of the obstacles too complex to reach the target

Another interesting observation regarding the detection radius variable is that when fixed at 0.1km, the radius precisely surrounds the eVTOL. As figure 4.4 shows, the eVTOL is able to get very close to the obstacle during its trajectory and to avoid it. It is the detection of the obstacle that is made at the last moment, without affecting the success rate of the mission, as shown in table 4.3.

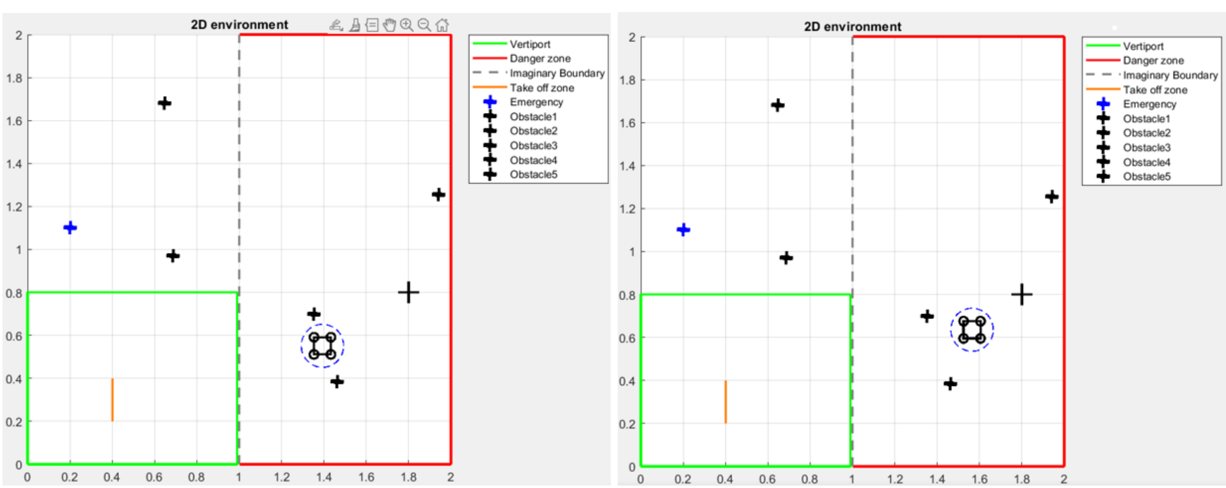

FIGURE 4.4 – Low sensor range enables optimised path

On the figure 4.4, it was possible for the eVTOL to pass through these two obstacles because its radius was so small. If it had been higher, as was the case for the rest of the simulations, it would not have followed the same trajectory. Therefore, setting the radius to a low value such as 0.1km brings us closer to an optimized trajectory, nearly comparable to that of the A* algorithm.

4.3 Naive algorithm

Once the detection radius had been set at 0.2km, the naive algorithm was tested with an eVTOL going to rescue a target with a number of obstacles varying from one to five. For each case, 200 simulations were carried out and the results are listed in the table 4.4. For each configuration, links to YouTube videos in the appendices illustrate how the naive algorithm works.

	Average time (s)	**Average success (%)**	**Standard deviation**
0 obstacle	21,42	100	0,27
1 obstacle	22,55	100	0,88
2 obstacles	23,78	100	1,83
3 obstacles	24,90	100	1,91
4 obstacles	26,72	99,5	2,88
5 obstacles	28,82	99,5	3,53

TABLE 4.4 – Time, success and standard deviation depending on the number of obstacles

The results obtained show a success rate close to 100% and a standard deviation which, like the average time, increases with the number of obstacles. This is coherent, since the more obstacles there are, the greater the number of emergency procedures, and the greater the number of obstacle avoidances, which increases path time.

By the way, it is very important to carry out the simulations with the same computer from start to finish, having optimised its active and inactive memory, otherwise the time will vary greatly. This is why the average simulation time is around 30 seconds, whereas all the YouTube videos are longer than 30 seconds.

4.4 A* algorithm

To draw a parallel with the naive algorithm, the same number of iterations were carried out and gave the following results which are listed in the table 4.5.

	Average time (s)	**Average success (%)**	**Standard deviation**
0 obstacle	21,42	100	0,27
1 obstacle	21,44	100	0,50
2 obstacles	21,75	100	0,57
3 obstacles	22,17	100	0,73
4 obstacles	23,05	99,5	0,86
5 obstacles	23,90	100	0,90

TABLE 4.5 – Time, success and standard deviation depending on the number of obstacles

Similarly, the statistics obtained show an average success close to 100% and a standard deviation which, like the average time, increases with the number of obstacles, but much slower than the naive algorithm.

4.5 Overall results

In order to better compare the results between the two algorithms, it is interesting to see the average path times as a function of the number of obstacles. Thanks to tables 4.4 and 4.5, the five points obtained per algorithm were used to perform a linear regression, obtaining two line equations with a correlation coefficient close to 1. It is also worth noting that the steering coefficient of the naive algorithm is almost three times greater than that of the A* algorithm.

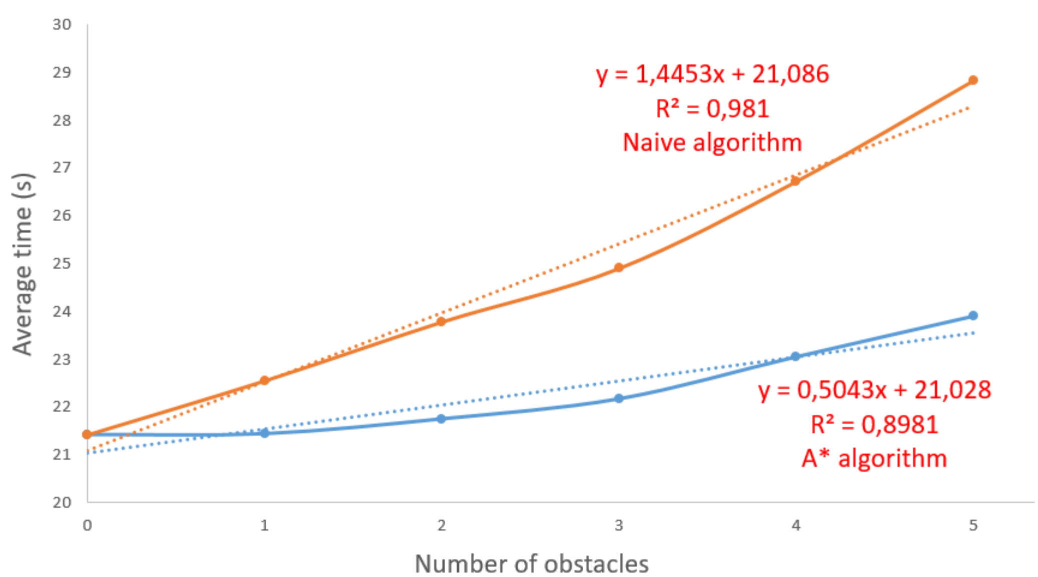

FIGURE 4.5 – Average time as a function of number of obstacles with a linear approximation

Even if the correlation coefficient is close to 1, another interesting approximation would be a quadratic one, which enables to get a correlation coefficient much closer to 1, such as suggested in figure 4.6.

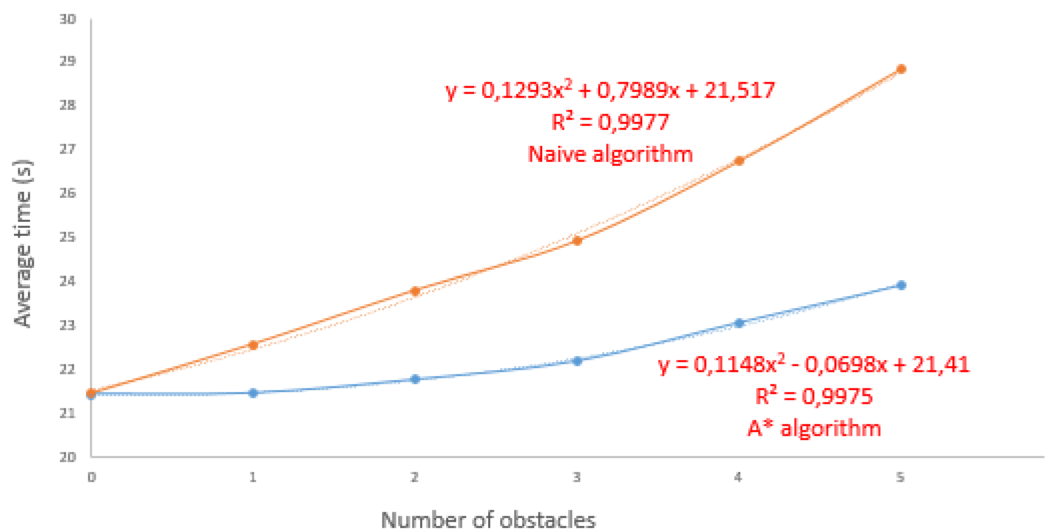

FIGURE 4.6 – Average time as a function of number of obstacles with a quadratic approximation

Similarly, the standard deviation, as shown in figure 4.7, is an interesting parameter to study. The standard deviation allows us to measure the dispersion of the values obtained by all the simulations. In this case, a linear regression made it possible to obtain line equations whose coefficient is also close to 1. Here, the same observation as for figures 4.5 and 4.6, the directing coefficient is five times higher for the naive algorithm than for the A* algorithm, which is consistent with the emergency protocol which disperses the values more easily.

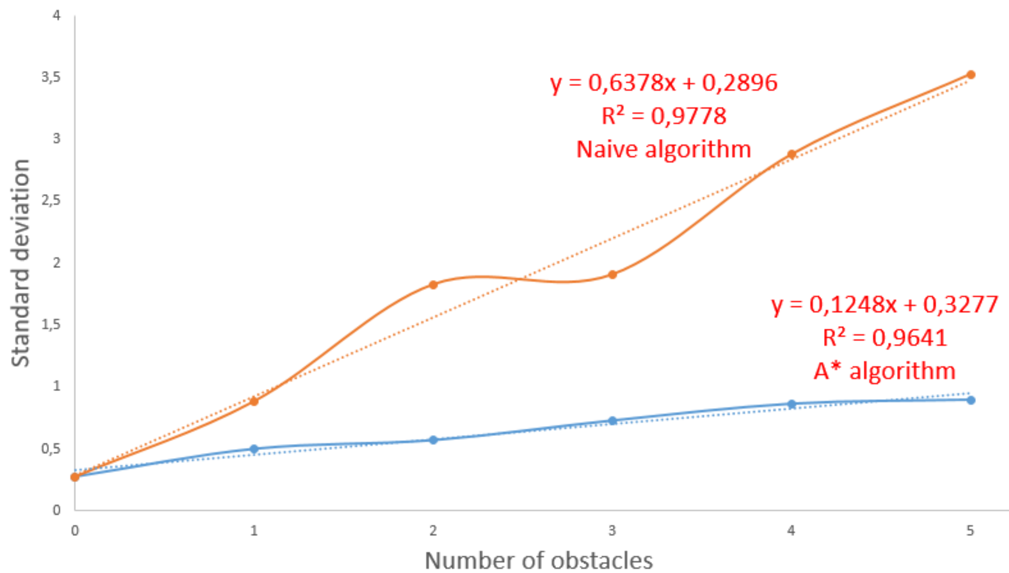

FIGURE 4.7 – Standard deviation as a function of number of obstacles

4.6 Multiple eVTOLs

Since the naive algorithm seems quite efficient even if it can be optimized, simulations were carried out with multiple eVTOLs to highlight the notion of priority when two eVTOLs have different routes illustrating the idea for one eVTOL to avoid another one, which means in another terms, a dynamic avoidance.

A notable result concerning the notion of priority is observed at the beginning of the outward path. It was defined that the eVTOL furthest away departs first, with the second departing once the first exits its detection radius. As a result, the first eVTOL departs in a direction that not only suits it but also does not interfere with the second eVTOL, which will head towards its target afterward, as shown in figures 4.8 and 4.9.

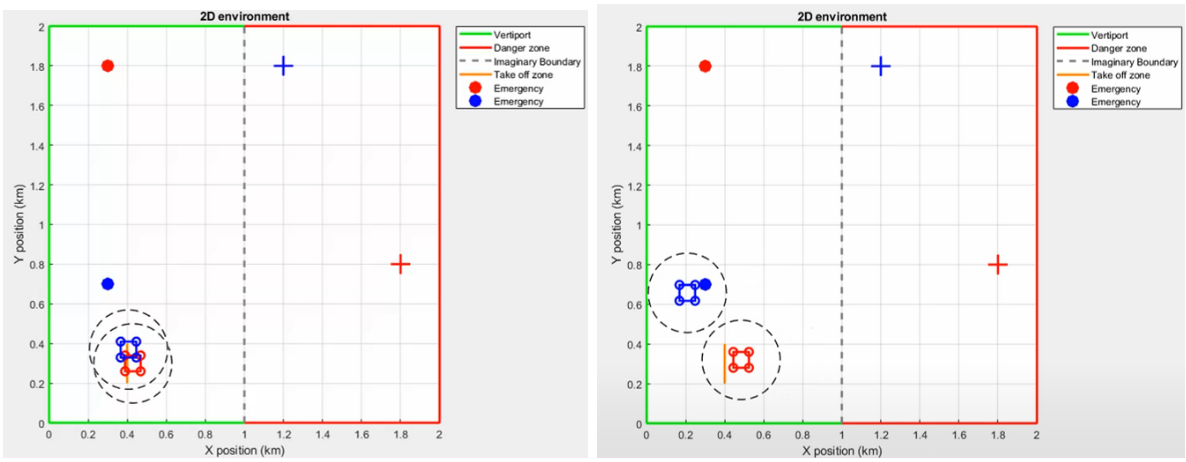

FIGURE 4.8 – Priority from blue eVTOL over red eVTOL on the outward path

After picking up their respective targets, the two eVTOLs in figure 4.9 will inevitably intersect, but the blue one, being closer to its hospital, will have priority over the red one, which will let it pass. Indeed, it can be seen in the first photo below that it waits for the blue one to pass before continuing its path.

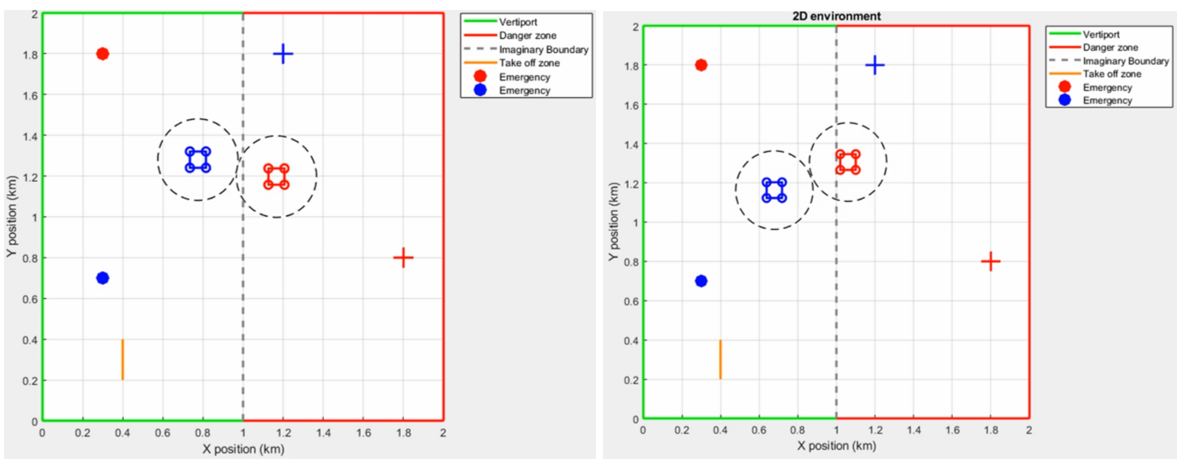

FIGURE 4.9 – Priority from blue eVTOL over red eVTOL on the return path

In reality, in the developed model, an eVTOL will consider another eVTOL as a dynamic obstacle and will act to avoid it by checking at each iteration if it enters its detection radius.

4.7 Application to a concrete scenario

Considering the scenario detailed earlier, the presence of 32 obstacles on a possible path connecting the international airport and the Bondi Junction shopping center has been estimated.

Before applying linear regression, it is important to note that the Matlab environment for the naive algorithm was designed to ensure that the eVTOL's speed was feasible. Thus, it was decided to construct a square with sides of 2 kilometers. By doing so, the average distance traveled by an eVTOL was approximately four kilometers. In our case study, the international airport is about 8 kilometers in a straight line from the shopping center, so the entire function must be multiplied by two.

Thus, applying the previously determined linear regression formula, the estimated required travel time is 134.67 seconds, or 2 minutes and 14 seconds, with linear estimation, while quadratic estimation yields a result of 358.97 seconds, or 5 minutes and 58 seconds.

In contrast, by applying the A* algorithm, the travel time is 67.04 seconds, or approximately 1 minute and 7 seconds for a linear approximation. For a quadratic approximation, the travel time is 270.58 seconds, or approximately 4 minutes and 30 seconds.

The summary of the results for the time travel is presented in the table below :

	Naive algorithm	**A* algorithm**
Linear	134.67s	67.04s
Quadratic	358.97s	270.58s

TABLE 4.6 – Time travel according the algorithm and the approximation

Consequently, the average speed is calculated and can be compared to the eVTOL presented in the section 3.3.1 with a maximum speed of 300km/h :

	Naive algorithm	**A* algorithm**	**Efficiency difference**
Linear	214 km/h	431 km/h	101 %
Quadratic	80 km/h	107 km/h	34 %

TABLE 4.7 – Average speed according to the algorithm and the approximation

Table 4.7 presents the efficiency difference between the A* algorithm and the naive algorithm varies by 34% and 101%.

5 Discussion

This section discusses the research's significance and contributions to the field, summarizes the findings, and relates them to the research questions and hypotheses. It also discusses the limitations of the study.

5.1 Summary and analysis of the results

The results presented the Shapiro-Wilk test in the section 4.1, enabled to compare different simulations since they follow more or less strongly normal distributions. Indeed, the test gives us p-values whose interpretation can lead to different interpretations and different choices of acceptance or rejection of hypotheses. In our case, it was considered that the p-values were sufficient overall, although for the naive algorithm, the more obstacles there were, the less the p-value tended to follow a normal distribution. However, it is important to consider that among the thousands of simulations, outlier values may be obtained, which can skew the results. Hence the acceptance of the hypothesis that the distributions follow a normal law, more or less strongly. Consequently, the results of this test enable to compare more legitimately the two algorithms.

Regarding the results in the section 4.2, the naive model was based on a counter that increments each time the detection radius contacts an obstacle. The counter was set to 50, and it turns out that this allows for coherent and feasible results. Furthermore, through thousands of simulations, the detection radius was set to 0.2 km, although it could have been set to 0.1 km for more optimization. This choice is debatable but justified by the naive aspect. Indeed, it would not have been consistent to set it too high since the objective was to create a credible model, so it had to be set in such a way that the mission success rate is high while maintaining a certain number of emergency procedures.

The results concerning the naive algorithm presented in the section 4.3 show that the emergency protocol allows for taking a safety altitude, which is close to what could happen in a mission with a helicopter, so it does not pose a problem in terms of credibility. However, the naive algorithm then takes a new random position, and this choice is debatable. Indeed, in real life, if a helicopter hits an obstacle or trajectory multiple times, it can take altitude to move onto a new trajectory but will not necessarily move to the other end of the map. A possible response would be the naive nature of the algorithm whose primary objective is not the optimization of the trajectory, but the success of the mission. Additionally, an arbitrary threshold of 50 was chosen for trial and error because this value empirically seemed to best simulate what an eVTOL might do when attempting to bump against an obstacle by maneuvering around it a certain number of times before giving up and selecting another random position. If this threshold had been set lower, there would have been more emergency procedures, resulting in higher measurements. Conversely, the higher the threshold, the more the eVTOL would persist in trying to evade the obstacle at all costs, leading to fewer emergency procedures. However, it would have been interesting and possible to adjust the detection radius, which would allow for a trajectory more or less close to the obstacles, by varying this threshold to determine which configuration would have been the most optimal.

In contrast, in section 4.4, the A* algorithm is aimed at optimizing the trajectory. Therefore, when comparing the two models, it is evident that the standard deviation of the naive model increases five times faster than that of the optimized model, which aligns with the objectives of these models. Similarly, the same trend is observed concerning the evolution of the average travel time for each model, with the difference being that the factor distinguishing the two models is no longer five but three for the linear model, which confirms the efficiency of such an algorithm as proven in [29][33].

However, these approximations, whether linear or quadratic, should be nuanced as they only consist of five points each. Clearly, five points is quite a small number to estimate the true shape of a curve, even if the coefficient is close to 1. It would probably have been wiser to increase the number of obstacles to have more points, but since the code's complexity was already too high, it was decided not to focus on this to obtain other results.

Overall, both algorithms provide a very high success rate, close to 100%, which was the goal, particularly for the naive algorithm, in other terms, to be able to establish a credible model capable of responding to any possible scenario up to a point it has been possible to create a scenario with several eVTOLs able to save several targets such as presented in the section 4.6.

The section 4.6 presents promising results in a sense that different eVTOLs are enable to interact between them. Indeed, one eVTOL does not enter in the sensor range of the other and respect the rules of priority that have been defined in the section 3.7. However, there are a few minor bugs in the code, notably that the eVTOL that does not have priority waits until the other has finished moving. In fact, there are some small to-and-fro movements, as if at each iteration it tried to move forward again but realised that this was not possible because of the detection radius of the other eVTOL. This could therefore be due either to small display bugs or to a unit increment that is too high and can be seen by the naked eye, and the right value to fix this issue needs to be determined. In any case, it doesn't change the success of the mission, it just makes it slightly less fluid and reminds us of the naive aspect of the programme, which was developed to avoid obstacles with this principle of trial and error at each iteration.

Regarding the section 4.7 about the concrete case of the April 13, 2024, attack at the Bondi Junction shopping center, the results for the naive algorithm obtained vary significantly depending on the type of approximation used. Indeed, the time for a quadratic estimation is almost three times longer than for a linear estimation. For a distance of approximately 8 kilometers from Sydney Airport to the shopping center, the time taken by the eVTOL implies an average speed exceeding 80 km/h for a quadratic estimation, whereas the linear approximation implies an average speed of 214 km/h. Considering that the eVTOL model currently being developed in Sydney presented in figure 3.2 [24] is capable of reaching speeds up to 300 km/h, neither approximation should be excluded. However, when considering this average speed, it is important to account for obstacles, their detection time, and avoidance, which necessarily slow down the eVTOL compared to its cruising speed. Therefore, the possibility of maintaining 214 km/h seems relatively high when considering this factor and thus less credible than the quadratic approximation. Moreover, this is supported by the study of the correlation coefficient, which is much closer to 1 with a quadratic estimation than with a linear estimation. The same observation can be made with the A* algorithm, although with shorter times. Indeed, with a linear approximation, the travel time would be 67 seconds, which would correspond to an average speed of 431 km/h. This seems far too high, prompting the rejection of the linear approximation whose correlation coefficient was the lowest (0.89), whose the efficiency difference is 101%, which represents a significant margin, thus questioning the relevance of the naive algorithm. Conversely, with a quadratic approximation, the travel time would be 270 seconds, resulting in an average speed of 107 km/h, which appears to be a feasible and consistent speed given the obstacle avoidance maneuvers. Overall, the quadratic approximation seems much more credible which coherent with the correlation coefficient, closer to 1 whose the efficiency difference is only 34%, indicating a relatively small margin, thus justifying the relevance of such a naive algorithm.

Nonetheless, in all cases, the speed is particularly high, confirming the utility and potential of such vehicles, which do not face the same urban constraints as conventional vehicles like fire trucks or ambulances.

5.2 Limitations

In spite of the fact the naive algorithm presented in this thesis seems to be promising, some limitations have to be taken into account to gain a broader perspective on the work done.

5.2.1 Environment modelling

Furthermore, to improve the model, it would be interesting to modify it to make it three-dimensional. This would provide an even better representation of reality and create an environment closer to that of an urban environment.

In this thesis, the environment has been simplified, by considering it as a square like in figure 3.1, whereas in real life, urban zones are much more complex than that, with forbidden zones, like jails, military, private zones which need to be taken in account in real life. Indeed, as specified in figure 2.7, the airspace is currently divided into different flight levels in altitude and zones at the same height. Consequently, the regulations are particularly complex to manage all these transfers, whether they are vertical across different flight levels or segmented zones. This is why, during a change in flight level or zones, it is required to obtain what is called a clearance to request authorization if needed. Therefore, in our study, these parameters are not taken into account contrary to [28], where those research try to integrate such Visual Flight Rules.

In addition, when several eVTOLs were going to rescue several targets, a random choice was made to launch them from the same place and land them on different hospitals as suggested in figure 3.10. In practice, it seems reasonable in large agglomerations to have several hospitals, as in the city of Sydney where the case study was taken. Nevertheless, it is true that it might also have been possible to have them take off from different locations and land at the same hospital.

5.2.2 Obstacles modelling

During the simulations, all the obstacles have been considered circular and with a more or less fixed radius. However, in an urban environment, obstacles can be symbolised in a multitude of ways : road signs, infrastructures, flows of people. In fact, it seems appropriate for a forthcoming thesis to take up this model again in order to approach an even more concrete case, which would provide even more convincing and significant results.

Besides, like described in [35], the obstacles have been considered firstly as static during the simulations whereas in reality, there are dynamic obstacles that can be found in the street such as people, cars or even aerodynamics effects. Only dynamic obstacles were considered in a second phase, when multiple eVTOLs were modeled simultaneously. Indeed, each eVTOL regarded the other eVTOLs as dynamic obstacles that needed to be avoided in each iteration.

In our study, static and dynamic obstacle avoidance were examined separately, without reconciling the two simultaneously. Furthermore, our section on dynamic obstacle avoidance with multiple eVTOLs is very simplistic. Indeed, the major risks can occur during takeoff, landing, and when they cross paths on their trajectories. To mitigate these issues, it was decided that if one eVTOL detects another, the latter will stop until it is out of the detection radius. Consequently, the behavior of the eVTOL in avoiding dynamic obstacles effectively becomes static obstacle avoidance when the situation demands it.

5.2.3 eVTOL modelling

In the naive algorithm, the eVTOL is assumed to be unaware of the location of obstacles, even though it could potentially be aware of them in advance of the mission. In addition, the obstacle detection radius has been chosen so that the safety protocol is activated intelligently and not too frequently like in figure 4.3 where the sensor is definitely too large. The promising side of the algorithm would not have been so present if a larger radius had initially been chosen, as shown in figure 4.3. The size of the eVTOL has also been chosen in order to be seen clearly whereas in reality its maximum longer would be around 10 meters.

Moreover, the sensor range of the eVTOL was considered to be working all the time whereas air quality or urban noises can affect them. In addition, it can also reduce visibility due to smog or suspended particles can complicate navigation and collision avoidance.

It would also be interesting to implement a cost function in the eVTOL instead of a detection circle. Here, the eVTOL only changes its trajectory when its detection circle encounters the obstacle, so its reaction is a boolean, either true or false. In reality, however, incorporation of a cost function would be necessary, the variables of which would be a linear combination of several factors that would influence its trajectory, so that its trajectory would be influenced slightly in order to make the eVTOL's reaction not naive this time, but more intelligent and adaptable.

5.2.4 Code and software

In the naive model, it is possible to improve the code as such to simplify it by adding classes and functions to avoid repeating blocks of code that would make it cumbersome and complicated. Indeed, the software sometimes crashes or stalls, mainly because the complexity of the code is so quite high because not enough optimised. In the same vein, to facilitate simulations, it might have been more effective to create the model using software other than Matlab, which sometimes quickly shows its limits in terms of simulation power and sometimes generates display problems like on figure 4.4. Thus, developing such a model could be perhaps more interesting on C+ for instance.

6 Conclusion

This section provides recommendations for future research and applications of the study, and it concludes on the research conducted and its implications for eVTOLs trajectories in urban environment.

6.1 Scope for further research

As previously discussed, even though promising the work done in this thesis is constrained by limiting factors and future work should be focused on the following points which could add great improvement and accuracy to the model already developed.

Furthermore, the different scenarios that have been selected do not necessarily take into account all the possible scenarios. In our case, as explained in the section 3.7 a decision was made to adopt a relatively simplistic scenario with just two priority rules, one for the outward path and another for the return path. In reality, the conditions of a mission can vary greatly and there may be other factors to take into account as developed in [25][36].

For example, no specific study has been made of the influence of certain aerodynamic factors in an urban environment, such as wind variations are crucial to consider. Wind shear, which corresponds to variations in wind speed and direction over short distances, can cause instability. In addition, gusts of wind, sudden and brief increases in wind speed, as well as turbulence generated by urban structures, can have a significant impact on stability and flight control.

Furthermore, urban obstacles, such as buildings, trees and other structures, also influence airflow like explained in [34]. These structures can create wind tunnels, vortices and wake turbulence. Tall buildings, in particular, can channel the wind through streets, increasing wind speed and creating urban canyon effects. In narrow streets and between nearby buildings, the wind can be accelerated, a phenomenon known as the Venturi effect. In addition, eddies can form at the corners of buildings and at intersections, creating additional challenges for the navigation and stability of airborne vehicles.

Besides, thermal conditions in urban areas also play an important role. Urban heat islands, where temperatures are higher than in the surrounding rural areas, affect air density and, consequently, aircraft lift. In addition, differential solar heating of urban surfaces can generate thermal updrafts and downdrafts, disrupting flight paths.

Moreover, as precised in the section before, it is crucial to consider the third dimension in order to take into account the rolling and pitching effects of the eVTOL as it performs its trajectory. The two-dimensional model does not take this into account. However, as an eVTOL has rotors like a drone or helicopter, it is necessary to consider these movements, particularly with trajectories such as Dubins trajectories like in [32]. Indeed, a Dubins trajectory is the shortest trajectory that a vehicle can follow while respecting a minimum turn constraint. The naive algorithm would therefore need to implement such a programme with a minimum turning radius to ensure obstacle avoidance for safety in an urban environment and to avoid an accident.

Furthermore, in the experimental conditions of the naive algorithm and the A* algorithm, it was decided to set certain variables randomly and others deterministically. It would have been just as appropriate to fix on a single map, a single case study, in order to be able to study more algorithms in greater detail and seek to optimise the trajectory even further in this environment. Certainly, confining ourselves to a singular environment would have enabled the utilization of various correctors, which could have been implemented in the code to conduct a more detailed study of trajectories.

All those conditions, haven't been taken in account in this thesis and deserve also specific research on it with more complex scenarios, in order to avoid some unwanted effects such as pure roll or dutch roll or everything that could compromise the safety of the mission and cover a wider range of possible scenarios.

6.2 Contribution of the thesis

This thesis draws its interest from the fact that scientific research on urban rescue by eVTOLs was relatively scarce while urban areas are expanding and becoming more complex due to population growth. It was therefore essential to find a way to ensure the flight safety of eVTOLs during the trajectories they perform, as well as the safety of the victims that need to be rescued, especially in a world where threats are becoming multifactorial.

This research has made the following explicit contributions to the field of eVTOLs' paths in urban environment for rescue missions :

1. Creation a credible environment and scenario
2. Development a naive algorithm with a high rate success
3. Comparison between the naive algorithm and the A* one
4. Extension of this idea with multiple eVTOLs rescuing multiple targets.
5. Application of the algorithm to a recent concrete case.

Although this research primarily adopts a theoretical framework through simulation, it lays the foundation for eVTOLs' paths in urban environment for rescue missions, especially with the naive algorithm that looks promising even if its trajectory can be optimised, it does not discredit the naive model. Therefore, to confirm such a model, concrete applications are needed, such as the Vertiia eVTOL developed at Bankstown airport in Sydney, with which some researchers of the University of Sydney are in frequent contact.

7 Bibliography

[1] Urbanization | Population division. (s. d.). https://www.un.org/development/desa/pd/content/urbanization-0

[2] Statista. (2023, 18 octobre). Population growth of largest global megacities 2000-2035. https://www.statista.com/statistics/911964/population-growth-of-the-major-urban-cities/

[3] Injury in Australia : Transport accidents. (2023, 6 juillet). Australian Institute Of Health And Welfare. https://www.aihw.gov.au/reports/injury/transport-accidents

[4] World Health Organization : WHO. (2021, 11 juin). Maladies cardiovasculaires. https://www.who.int/fr/news-room/fact-sheets/detail/cardiovascular-diseases-(cvds)

[5] National Library of Medecine https://www.ncbi.nlm.nih.gov/pmc/articles/PMC10808805/

[6] Bushfire | Community Safety | Geoscience Australia. (s. d.). https://www.ga.gov.au/scientific-topics/community-safety/bushfire

[7] Labib, N. S., Danoy, G., Musial, J., Brust, M. R., Bouvry, P. (2019). Internet of Unmanned Aerial Vehicles—A Multilayer Low-Altitude Airspace Model for Distributed UAV Traffic Management. Sensors, 19(21), 4779. https://doi.org/10.3390/s19214779

[8] Sunil, E., Ellerbroek, J., Hoekstra, J., Vidosavljevic, A., Arntzen, M., Bussink, F., et al. (2016). Analysis of airspace structure and capacity for decentralized separation using fast-time simulations. J. Guid. Control Dyn. 40 (1), 38–51.

[9] A.Smirnov. Problems and Prospects for the Development of Urban Airmobility on the Basis of Unmanned Transport Systems. https://www.sciencedirect.com/science/article/pii/S2352146523000224

[10] Guzmán, J., Baeza, V. M. (2023). Enhancing Urban Mobility through Traffic Management with UAVs and VLC Technologies. Drones, 8(1), 7. https://doi.org/10.3390/drones8010007

[11] R.Berger. The rise of a new mode of transportation. Urban Air Mobility 5.

[12] National Academies. Science Engineering Medecine. Stochastic Vehicle-Queue-Load Model For Large Bridges. https://trid.trb.org/view/409776

[13] Shrestha, R., Oh, I., Kim, S. (2021b). A Survey on Operation Concept, Advancements, and Challenging Issues of Urban Air Traffic Management. Frontiers In Future Transportation, 2. https://doi.org/10.3389/ffutr.2021.626935

[14] Adminwcr. (2022, 19 mai). Commercial Uses and Applications of Drones. AUAV. https://www.auav.com.au/articles/what-is-a-drone-used-for/

[15] N. Muchiri, S. Kimathi (2016, 4 mai). A Review of Applications and Potential Applications of UAV https://sri.jkuat.ac.ke/jkuatsri/index.php/sri/article/view/325/301

[16] Wang, Z., Wong, K. (2019). Autonomous Pest Bird Deterring for Agricultural Crops Using Teams of Unmanned Aerial Vehicles. https://dblp.uni-trier.de/db/conf/ascc/ascc2019.html#WangW19

[17] Tuśnio, N., Wróblewski, W. (2021). The Efficiency of Drones Usage for Safety and Rescue Operations in an Open Area : A Case from Poland. Sustainability, 14(1), 327. https://doi.org/10.3390/su14010327

[18] How Helicopters Aid Search and Rescue and Disaster Relief Missions | Helicopter Express. (s. d.). https://www.helicopterexpress.com/blog/helicopter-search-and-rescue

[19] Matrice 300 RTK - Industrial grade mapping inspection drones - DJI Enterprise. (s. d.). DJI. https://enterprise.dji.com/matrice-300

[20] Phantom 4 Pro v2.0 - DJI. (s. d.). DJI Official. https://www.dji.com/au/phantom-4-pro-v2

[21] Home | AMSL Aero Pty Ltd. (s. d.). Vertiia. https://www.amslaero.com/

[22] Biba, J. (2023, 1 juin). What Are eVTOLs ? Are They the Future of Aviation ? Built In. https://builtin.com/articles/evtol-aircraft

[23] Doo, Pavel, Didey, Hange. (August 2021) NASA Electric Vertical Takeoff and Landing (EVTOL) aircraft technology for public services – a white paper. NASA Transformative Vertical Flight Working Group 4 (TVF4)

[24] Advanced Air Mobility Mission - NASA. (s. d.-b). NASA. https://www.nasa.gov/mission/aam/

[25] Liu, H., Ge, J., Wang, Y., Li, J., Ding, K., Zhang, Z., Guo, Z., Li, W., Lan, J. (2021). Multi-UAV Optimal Mission Assignment and Path Planning for Disaster Rescue Using Adaptive Genetic Algorithm and Improved Artificial Bee Colony Method. Actuators, 11(1), 4. https://doi.org/10.3390/act11010004

[26] eVTOL Arrival Sequencing and Scheduling for On-Demand Urban Air Mobility. (2018b, septembre 1). IEEE Conference Publication | IEEE Xplore. https://ieeexplore.ieee.org/abstract/document/8569645

[27] National Aeronautics and Space Administration. (2020, November). Advanced Air Mobility (AAM) Vertiport Automation Trade Study

[28] Feasibility Study of Operation Volume Design Concept for Integration of Aircraft Flying Under Visual Flight Rules Based on Actual Flights. (2023, 1 juin). IEEE Journals Magazine | IEEE Xplore. https://ieeexplore.ieee.org/abstract/document/10049067

[29] Ye, M., Zhao, J., Guan, Q., Zhang, X. (2024). Research on eVTOL Air Route Network Planning Based on Improved A* Algorithm. Sustainability, 16(2), 561. https://doi.org/10.3390/su16020561

[30] Habibi, H., Safaei, A., Voos, H., Darouach, M., Sánchez-López, J. L. (2023). Safe navigation of a quadrotor UAV with uncertain dynamics and guaranteed collision avoidance using barrier Lyapunov function. Aerospace Science And Technology, 132, 108064. https://doi.org/10.1016/j.

ast.2022.108064

[31] Path Planning and Tracking Control Method Based on Bessel Curve. (2022b, novembre 18). IEEE Conference Publication | IEEE Xplore. https://ieeexplore.ieee.org/abstract/document/10021359

[32] Path planning using 3D Dubins Curve for Unmanned Aerial Vehicles. (2014b, mai 1). IEEE Conference Publication | IEEE Xplore. https://ieeexplore.ieee.org/abstract/document/6842268

[33] An Improved A* Algorithm for UAV Path Planning Problems. (2020, 1 juin). IEEE Conference Publication | IEEE Xplore. https://ieeexplore.ieee.org/abstract/document/9084806

[34] Bilgin, Z., Yavrucuk, İ., & Bronz, M. (2024). Urban Air Mobility Guidance with Panel Method : Experimental Evaluation Under Wind Disturbances. Journal Of Guidance, Control, And Dynamics, 1-17. https://doi.org/10.2514/1.g007691

[35] Sampling-Based Path Planning for UAV Collision Avoidance. (2017, 1 novembre). IEEE Journals & Magazine | IEEE Xplore. https://ieeexplore.ieee.org/abstract/document/7911207

[36] Baker, C., Ramchurn, G., Teacy, L., Jennings, N. (2016). Planning search and rescue missions for UAV teams. Planning Search And Rescue Missions For UAV Teams, 1777-1782. https://doi.org/10.3233/978-1-61499-672-9-1777

8 Appendices

8.1 Python code for Shapiro-Wilk test

```python
import numpy as np
from scipy import stats

1 usage
def shapiro_wilk_test(data):
    # Effectuer le test de Shapiro-Wilk
    stat, p_value = stats.shapiro(data)
    if p_value > 0.10:
        classification = "Very high"
    elif 0.10 >= p_value > 0.05:
        classification = "Moderately high"
    elif 0.05 >= p_value > 0.01:
        classification = "Medium"
    elif 0.01 >= p_value > 0.001:
        classification = "Low"
    else:
        classification = "Very low"

    return stat, p_value, classification


data = 'remplacer par la colonne à considérer'

stat, p_value, classification = shapiro_wilk_test(data)

print(f'Statistic: {stat}')
print(f'P-value: {p_value}')
print(f'Probability of following a normal distribution: {classification}')
```

FIGURE 8.1 – Python code for Shapiro-Wilk test

8.2 Excel table of simulations

8.2.1 Naive algorithm : accurate sensor range

	A	B	C	D	E	F	G	H	I	J
1	R=	0,1	R=	0,2	R=	0,3	R=	0,4	R=	0,5
2	Time	Success	Time	Success	Time	Success	Time	Success	Time	Success
3	22,92	1	26,87	1	25,02	1	40,72	1	50,38	1
4	23,25	1	22,55	1	33,97	1	48,04	1		0
5	23,43	1	29,24	1	26,87	1	47,93	1	42,63	1
6	22,2	1	33,64	1	28,11	1	28,9	1	55,68	1
7	21,98	1	26,8	1	33,78	1	45,76	1	47,16	1
8	24,48	1	26,93	1	36,63	1	26,4	1	72,11	1
9	23,85	1	27,28	1	38,17	1	27,19	1	36,32	1
10	24,18	1	30,09	1	40,78	1		0		0
11	22,61	1	28,03	1	46,24	1	30,97	1	63,9	1
12	24,71	1	28,88	1	30,29	1	41,32	1		0
13	24,06	1	26,5	1	25,43	1	30,56	1		0
14	23,14	1	29,32	1	25,02	1	38,72	1	36,5	1
15	25,39	1	30,89	1	34,25	1	41,81	1		0
16	25,06	1	28,45	1	37,45	1	40,66	1	61,96	1
17	22,75	1	31,96	1	29,72	1	38,13	1	47,26	1
18	23,68	1	27,03	1	25,02	1	51,2	1		0
19	23,28	1	25,07	1		0	28,22	1		0
20	22,53	1	27,33	1	34,28	1	40,01	1	57,61	1
21	24,31	1	27,69	1	36,62	1		0		0
22	24,41	1	25,79	1	27,14	1		0		0
23	22,92	1	29,87	1	42,18	1	32,34	1	52,69	1
24	22,35	1	24,61	1	37,26	1	47,25	1	60,46	1
25	24,13	1	23,62	1		0	31,08	1		0
26	24,81	1	25,31	1	43,91	1	53,1	1	60,28	1
27	21,02	1	28,41	1	43,56	1	33,82	1		0
28	22,18	1	28,49	1	31,64	1	62,65	1	52,31	1
29	22,38	1	27,22	1	32,35	1	40,13	1	33,42	1
30	25,91	1	26,26	1	50,43	1	44,49	1	35,57	1
31	23,24	1	30,67	1	37,99	1	37,02	1	43,28	1
32	23,12	1	30,05	1	39,59	1	41,59	1		0
33	26,2	1	27,99	1	25,26	1		0		0
34	24,46	1	31,47	1	25,02	1		0		0
35	24,33	1	23,28	1	31,82	1		0	50,41	1
36	24,39	1	32,71	1	39,57	1		0	61,91	1
37	22,35	1	28	1	25,51	1	40,71	1	55,46	1
38	21,77	1	31,46	1		0		0	53,68	1
39	23,21	1	32,07	1	26,19	1	48,06	1		0
40	25,17	1	22,55	1	44,44	1	38,22	1		0
41	24,05	1	26,97	1	37,64	1	40,78	1	59,04	1
42	24,16	1	35,07	1	39,06	1	47,15	1		0
43	23,53	1	27,87	1	44,53	1	40,02	1	61,86	1
44	23,67	1	26,69	1	48,64	1	59,88	1		0
45	23,33	1	34,5	1	46,44	1	41,92	1		0
46	24,03	1	25,56	1	25,02	1	25,02	1		0
47	23,61	1	35,03	1		0	46,76	1	46,53	1
48	24,04	1	26,13	1	29,04	1	45,8	1	70,54	1
49	22,34	1	32,31	1	40,82	1		0		0
50	25,36	1	26,03	1	46,29	1	54,1	1	47,89	1
51	22,47	1	32,79	1	42,21	1	48,7	1	43,32	1
52	24,39	1	23,41	1	35,49	1	48,65	1		0
53	22,69	1	24,97	1	25,02	1	41,83	1	45,37	1
54	24,42	1	31,63	1	35,91	1	38,07	1		0
55	24,04	1	22,55	1	34	1	43,59	1		0
56	24,11	1	25,57	1	40,7	1	49,11	1		0
57	22,57	1	25,82	1	34,3	1		0	50,69	1
58	23,27	1	27,73	1	41,46	1	50,1	1		0
59	23,22	1	26,83	1	40,15	1	34,29	1	61,38	1
60	21,59	1	26,11	1	33,36	1	44,78	1		0
61	23,09	1	31,53	1	27,55	1	44,73	1		0
62	24,4	1	30,76	1	32,51	1	30,89	1	48,64	1
63	23,24	1	25,84	1	36,25	1	47,46	1	48,35	1
64	23,83	1	32,3	1	29,51	1	35,91	1		0
65	24,54	1	29,26	1	31,01	1		0		0
66	26,3	1	27,49	1	31,62	1	27,88	1	36,99	1
67	24,02	1	31,18	1	27,72	1	50,3	1		0
68	25,81	1	26,85	1	37,95	1		0		0
69	22,59	1	24,66	1	38,38	1	53,08	1		0
70	23,63	1	33,52	1	49,5	1	36,84	1	48,84	1
71	24,14	1	28,83	1	34,23	1	31,68	1		0
72	24,23	1	36,9	1	32,17	1	31,52	1		0
73	23,72	1	29,03	1	34,35	1		0		0
74	22,8	1	30,01	1	32,69	1		0		0
75	22,87	1	32,21	1	37,39	1	40,62	1	50,78	1
76	23,36	1	34,02	1	43,7	1	55,64	1	47,97	1
77	24,43	1	29,44	1	25,02	1	58,92	1		0
78	22,45	1	25,82	1	34,25	1	41,86	1	60,69	1
79	23,43	1	31,57	1	29,14	1	49,59	1	69,32	1
80	23,47	1		0	27,55	1	48,16	1		0
81	24,56	1	28,62	1	44,53	1	43,45	1		0
82	24,6	1	23,2	1	39,78	1	51,83	1		0
83	23,62	1	27,77	1	50,43	1	49,64	1		0
84	24,33	1	31,38	1	28,71	1	41,89	1	45,54	1
85	23,65	1	29,78	1	25,02	1		0		0
86	22,42	1	22,6	1	31,28	1	38,94	1	47,62	1
87	23,12	1	28,86	1	37,26	1	41,82	1	63,31	1
88	23,53	1	23,75	1	32,7	1	42,25	1	72,37	1
89	21,28	1	29,1	1	41,7	1	48,48	1	60,55	1
90	25,31	1	23,64	1	25,02	1	41,14	1	43,38	1
91	22,69	1	34,85	1	49,95	1	39,18	1	65,92	1
92	24,99	1	30,4	1	35,75	1	42,76	1		0
93	24,3	1	28,59	1	35,8	1	43,22	1		0
94	24,54	1	27,25	1	32,13	1		0		0
95	25,04	1	29,86	1	34,92	1		0	40,03	1
96	24,8	1	25,44	1	46,32	1	37,51	1		0
97	22,79	1	26,18	1		0	46,05	1	50,83	1
98	23,83	1	31,78	1	33,19	1	56,04	1		0
99	24,15	1	34,75	1	27,98	1	40,96	1	48,59	1
100	22,96	1	28,32	1	36,08	1	41,27	1		0
101	24,62	1	26,18	1	30,21	1		0	57,01	1
102	24,39	1	26,33	1	33,1	1	44,66	1		0
103	24,36	1	26,24	1	28,47	1	43,96	1		0
104	22,66	1	30,77	1	39,7	1	51,66	1	48,99	1
105	25,07	1	24,66	1	25,02	1	55,04	1		0
106	23,19	1	35,27	1	34,16	1	25,02	1	51,43	1
107	23,96	1	30,22	1		0	27,55	1	47,02	1
108	22,52	1	27,74	1	35,64	1	25,02	1	53,94	1
109	25,39	1	25,66	1	39,97	1	49,59	1		0
110	23,03	1	22,59	1	29,6	1	45,05	1	58,43	1
111	23,52	1	27,5	1	31,15	1	48,07	1		0
112	23,42	1	27,52	1	36,05	1	38,5	1		0
113	23,26	1	32,68	1		0		0		0
114	23,81	1	26,63	1	36,8	1	36,92	1		0
115	23,79	1	37,01	1	32,97	1	45,75	1	45,68	1
116	22,72	1	22,98	1	25,02	1	48,33	1		0
117	23,38	1	30,09	1	43,9	1	45,18	1		0
118	23,39	1	30,92	1	39,31	1	47,79	1		0
119	24,18	1	30,78	1	34,07	1	35,49	1		0
120	23,05	1	30,02	1	25,02	1	52,81	1		0
121	23,72	1	28,11	1	29,07	1	29,31	1		0
122	24,29	1	31,68	1	37,46	1	42,91	1	65,08	1
123	22,87	1	29,19	1	37,56	1	38,46	1		0
124	22,21	1	30,3	1	35,11	1	44,02	1		0
125	24,49	1	24,63	1	35,76	1	32,44	1	46,72	1
126	22,58	1	33,6	1	45,93	1		0		0
127	24,08	1	30,55	1		0	26,4	1		0
128	22,85	1	32,56	1	34,01	1	33,98	1		0
129	22,71	1	36,25	1		0	26,65	1		0
130	23,22	1	26,58	1		0	36,51	1	63,34	1
131	22,73	1	29,83	1		0	54,05	1		0
132	24,27	1	32,61	1	50,24	1		0	48,5	1
133	24,72	1	31,56	1	37,81	1	34,58	1		0
134	23	1	22,55	1	33,32	1	25,02	1	56,35	1
135	23,74	1	29,47	1	27,01	1	50,25	1	54,57	1
136	23,48	1	30,03	1	41,05	1	34,04	1		0
137	23,84	1	29,98	1	32,15	1	42,06	1	61,67	1
138	23,31	1	30,21	1	34,88	1	38,6	1	61,1	1
139	21,02	1	25,32	1		0	46,91	1	44,62	1
140	22,56	1	32,72	1	32,45	1	45,24	1	37,97	1
141	21,96	1	31,92	1	37,99	1	43,78	1	50,23	1
142	21,99	1	26,78	1	33,75	1	42,35	1	62,09	1
143	25	1	29,35	1	38,05	1	45,54	1		0
144	26,7	1	32,18	1	25,75	1	37,64	1		0
145	22,08	1	29,87	1		0	41,58	1	47,67	1
146	24,87	1	25,49	1	37,95	1		0	48,07	1
147	23,77	1	31,48	1	33,38	1	39,99	1		0
148	26,03	1	30,65	1	31,25	1	50,62	1	49,34	1
149	24,95	1	32,49	1	27,43	1	31,51	1	55,07	1
150	23,14	1	22,55	1	33,94	1	37,58	1		0
151	23,96	1	26,08	1	44,54	1	40,29	1	36,26	1
152	24,26	1	27,47	1	36,55	1	44,7	1	46,59	1
153	23,22	1	26,57	1	29,64	1		0	62,21	1
154	22,98	1	22,55	1	33,24	1	45,97	1	34,48	1
155	22,15	1	28,32	1	41,75	1	27,99	1	65,03	1
156	24,9	1	32,8	1	34,14	1	63,07	1	33,42	1
157	24,73	1	38,45	1	32,36	1	27,95	1		0
158	24,5	1	36,31	1	41,74	1	48,19	1		0
159	24,63	1	28,93	1	32,24	1	42,19	1	51,27	1
160	22,61	1	30,12	1	33,9	1		0	39,43	1
161	22,84	1	32,89	1	41,37	1	36,11	1		0
162	23,22	1	32,42	1	40,27	1	42,02	1	39,77	1
163	24,11	1	22,55	1	32,82	1	49,49	1	54,27	1
164	24,91	1	28,97	1	34,49	1	40,44	1		0
165	24,18	1	35,2	1	27,89	1	48,93	1		0
166	24,33	1	28,22	1	45,85	1	53,35	1		0
167	23,36	1	30,93	1	34,44	1		0		0
168	24,54	1	29,29	1	37,52	1	27,47	1		0
169	23,5	1	22,55	1	38,67	1	51,22	1	63,01	1
170	25,2	1	27,61	1	37,03	1	43,39	1	44,91	1
171	25,58	1	30,31	1	41,66	1	32,71	1	46,94	1
172	23,22	1	28,18	1	47,28	1		0		0
173	24,74	1	24,51	1	36,19	1	45,54	1	42,18	1
174	24,23	1	35,61	1	29,69	1	46,22	1	51,2	1
175	22,59	1	25,49	1	28,32	1	41,92	1	41,75	1
176	22,44	1	26,97	1	35,14	1	58,31	1		0
177	23,18	1	29,21	1	28,53	1		0	56,14	1
178	23,24	1	22,55	1	29,94	1	39,21	1		0
179	22,94	1	31,92	1	43,75	1		0		0
180	23,59	1	24,75	1	43,22	1	49,57	1	55,67	1
181	24,33	1	32,17	1		0	38,3	1		0
182	25,26	1	22,55	1		0	52,51	1	66,4	1
183	25,76	1	28,16	1	35,85	1	40,75	1		0
184	24,2	1	25,1	1	30,86	1	49,55	1	51,06	1
185	24,79	1	23,69	1	27,38	1		0	53,03	1
186	23,16	1	30,57	1	25,02	1	40,65	1	61,87	1
187	23,58	1	23,96	1	41,5	1	43,89	1	48,57	1
188	21,66	1	32,03	1	35,06	1	45,56	1	38,4	1
189	24,25	1	34,06	1	34,87	1	36,78	1		0
190	23,63	1	37,24	1	37,59	1	38,5	1	70,88	1
191	24,06	1	27,13	1	32,57	1	45,35	1		0
192	23,88	1	31,94	1	31,42	1	50,96	1	44,04	1
193	23,97	1	30,38	1	30,21	1	37,21	1	49,11	1
194	22,84	1	30,37	1		0		0		0
195	24,81	1	31,13	1	34,21	1	51,56	1		0
196	23,35	1	34,8	1	30,58	1	41,37	1		0
197	22,83	1	28,35	1	43,49	1	49,52	1		0
198	23,25	1	27,29	1	38,56	1	41,08	1	51,71	1
199	23,61	1	24,6	1	32,28	1	47,11	1	52,68	1
200	24,46	1	27,64	1	36,18	1	48,36	1	54,7	1
201	21,92	1	27,48	1	36,04	1	49,85	1		0
202	23,98	1	29,47	1	38,74	1	49,24	1		0

FIGURE 8.2 – First draft of simulations : 1000 iterations with different sensor ranges

8.2.2 Naive algorithm : one eVTOL for one target with obstacles

	A	B	C	D	E	F	G	H	I	J	K	L
1	0 obstacle		1 obstacle		2 obstacles		3 obstacles		4 obstacles		5 obstacles	
2	Time	Success	Time	Success	Time	Success	Time	Success	Time	Success	Time	Success
3	21,32	1	21,52	1	22,1	1	25,75	1	23,63	1	26,87	1
4	21,41	1	23	1	22,13	1	24,98	1	25,23	1	22,55	1
5	21,1	1	24,17	1	24	1	23,03	1	27,17	1	29,24	1
6	21,66	1	21,6	1	28,06	1	26,28	1	22,96	1	33,64	1
7	21,31	1	21,13	1	20,5	1	21,88	1	24,52	1	26,8	1
8	21,46	1	22,02	1	26,87	1	24,6	1	27,93	1	26,93	1
9	21,33	1	21,11	1	20,45	1	26,33	1	25,29	1	27,28	1
10	21,08	1	21,45	1	24,05	1	23,47	1	25	1	30,09	1
11	21,79	1	21,47	1	23,09	1	27,03	1	26,76	1	28,03	1
12	21,31	1	24,13	1	22,48	1	25,49	1	24,69	1	28,88	1
13	21,26	1	20,93	1	20,45	1	23,82	1	27,07	1	26,5	1
14	21,92	1	22,64	1	25,24	1	22,69	1	26,93	1	29,32	1
15	21,56	1	24,06	1	24,31	1	26,44	1	24,8	1	30,89	1
16	21,12	1	22,87	1	20,45	1	25,36	1	28,46	1	28,45	1
17	21,98	1	23,19	1	26,52	1	27,27	1	30,55	1	31,96	1
18	21,72	1	22,01	1	22,24	1	25,93	0	27,87	1	27,03	1
19	21,69	1	21,17	1	24,36	1	28,9	1	27,01	1	25,07	1
20	21,42	1	22,99	1	21,61	1	21,25	1	26,58	1	27,33	1
21	21,58	1	24,3	1	24,58	1	23,68	1	24,69	1	27,69	1
22	21,26	1	21,82	1	20,45	1	25,21	1	27,09	1	25,79	1
23	21,7	1	21,63	1	22,78	1	21,84	1	26,87	1	29,87	1
24	21,84	1	23,17	1	26	1	22,44	1	29,73	1	24,61	1
25	21,22	1	22,88	1	26,28	1	25,17	1	28,58	1	23,62	1
26	21,19	1	23,98	1	26,36	1	23,65	1	25,12	1	25,31	1
27	21,54	1	22,98	1	24,93	1	24,49	1	24,29	1	28,41	1
28	21,2	1	23,64	1	22,07	1	25,1	1	22,78	1	28,49	1
29	21,58	1	22,06	1	20,45	1	22,53	1	24,69	1	27,22	1
30	21,52	1	22,85	1	25,9	1	24,53	1	27,09	1	26,26	1
31	21,3	1	22,37	1	23,47	1	26,69	1	30,84	1	30,67	1
32	21,7	1	23,04	1	25,07	1	21,25	1	32,26	1	30,05	1
33	21,54	1	21,06	1	24,58	1	22,12	1	21,63	1	27,99	1
34	21,38	1	22,89	1	26,4	1	28,37	1	26,53	1	31,47	1
35	21,65	1	22,37	1	21,67	1	27,51	1	29,94	1	23,28	1
36	21,61	1	22,48	1	27,65	1	25,33	1	22,83	1	32,71	1
37	21,41	1	22,82	1	23,23	1	26,93	1	22,8	1	28	1

	A	B	C	D	E	F	G	H	I	J	K	L
38	21,96	1	22,49	1	22,02	1	29,3	1	28,06	1	31,46	1
39	21,48	1	20,4	1	26,34	1	23,31	1	25,09	1	32,07	1
40	21,22	1	22,98	1	22,1	1	24,46	1	27,17	1	22,55	1
41	21,09	1	21,73	1	21,66	1	26,18	1	21,55	1	26,97	1
42	21,21	1	21,58	1	24,96	1	26,37	1	24,03	1	35,07	1
43	21,24	1	22,74	1	23,53	1	28,28	1	26,7	1	27,87	1
44	21,37	1	21,2	1	24,48	1	26,76	1	30,97	1	26,69	1
45	21,42	1	21,44	1	24,32	1	24,31	1	21,55	1	34,5	1
46	21,98	1	23,65	1	22,71	1	23,65	1	27,74	1	25,56	1
47	21,59	1	22,43	1	21,54	1	26,51	1	24,02	1	35,03	1
48	20,94	1	21,52	1	22,25	1	26,8	1	26,36	1	26,13	1
49	21,9	1	23,61	1	23,78	1	26,47	1	30,62	1	32,31	1
50	21,08	1	21,97	1	24,64	1	23,21	1	28,95	1	26,03	1
51	21,54	1	23,92	1	24,37	1	23,53	1	28,62	1	32,79	1
52	21,42	1	22,45	1	23,09	1	23,78	1	23,58	1	23,41	1
53	21,1	1	23,99	1	24,61	1	27,39	1	27,81	1	24,97	1
54	21,39	1	23,46	1	24,49	1	27,09	1	22,96	1	31,63	1
55	21,57	1	22	1	23,4	1	24,58	1	28,5	1	22,55	1
56	21,77	1	22,63	1	20,45	1	24,02	1	23,71	1	25,57	1
57	21,37	1	22,86	1	24,19	1	25,11	1	29,23	1	25,82	1
58	21,18	1	22,03	1	26,67	1	25,03	1	21,55	1	27,73	1
59	21,32	1	22,36	1	22,91	1	26,92	1	28,14	1	26,83	1
60	21,52	1	22,73	1	23,67	1	27	1	29,36	1	26,11	1
61	21,41	1	22,82	1	24,06	1	23,18	1	28,35	1	31,53	1
62	21,8	1	22,82	1	25,66	1	25,61	1	23,12	1	30,76	1
63	20,81	1	23,55	1	26,2	1	23,91	1	28,88	1	25,84	1
64	21,27	1	22,48	1	24,15	1	26,11	1	28,41	1	32,3	1
65	21,5	1	21,91	1	20,45	1	27,01	1	29,36	1	29,26	1
66	21,39	1	21,81	1	22,36	1	25,63	1	23,63	1	27,49	1
67	21,52	1	21,13	1	24,59	1	24,78	1	26,11	1	31,18	1
68	21,25	1	22,7	1	23,38	1	25,49	1	26,95	1	26,85	1
69	20,68	1	21,83	1	21,23	1	21,25	1	27,32	1	24,66	1
70	21,46	1	22,65	1	20,45	1	26,33	1	30,96	1	33,52	1
71	21,74	1	24,28	1	21,81	1	23,82	1	25,76	1	28,83	1
72	21,45	1	22,19	1	24,72	1	24,98	1	29,05	1	36,9	1
73	21,16	1	22,23	1	25,72	1	22,46	1	31,26	1	29,03	1
74	21,27	1	22,97	1	27,78	1	24,05	1	21,55	1	30,01	1
75	22,12	1	23	1	21,64	1	23,59	1	25,21	1	32,21	1

	A	B	C	D	E	F	G	H	I	J	K	L
76	21,58	1	22,92	1	20,86	1	25,41	1	22,93	1	34,02	1
77	21,92	1	22,58	1	26,62	1	23,16	1	27,44	1	29,44	1
78	21,26	1	22,72	1	23,08	1	27,17	1	24,21	1	25,82	1
79	21,36	1	21,71	1	22,06	1	23,58	1	22,59	1	31,57	1
80	21,95	1	23,22	1	25,59	1	24,14	1	27,9	1		0
81	21,2	1	23,41	1	23,77	1	26,52	1	25,17	1	28,62	1
82	21,13	1	24,05	1	20,99	1	26,15	1	26,55	1	23,2	1
83	21,49	1	23,61	1	23,49	1	24,09	1	26,54	1	27,77	1
84	21,64	1	23,53	1	22,95	1	21,28	1	21,55	1	31,38	1
85	21,58	1	21,73	1	22,44	1	24,24	1	27,83	1	29,78	1
86	21,24	1	23,86	1	23,73	1	24,93	1	24,91	1	22,6	1
87	21,79	1	22,78	1	24,82	1	25,81	1	25,79	1	28,86	1
88	21,45	1	23,88	1	23,24	1	26,26	1	29,54	1	23,75	1
89	21,41	1	22,95	1	22,9	1	24	1	29,08	1	29,1	1
90	21,52	1	23,14	1	22,47	1	23,76	1	24,12	1	23,64	1
91	21,6	1	22,07	1	26,81	1	29,29	1	29,09	1	34,85	1
92	21,74	1	23,09	1	23,4	1	21,73	1	32,14	1	30,4	1
93	21,66	1	22,08	1	26,51	1	25,83	1	21,55	1	28,59	1
94	21,29	1	21,69	1	23,82	1	26,22	1	26,71	1	27,25	1
95	21,14	1	21,98	1	23,43	1	22,55	1	27,52	1	29,86	1
96	20,95	1	23,06	1	23,83	1	23,04	1	26,96	1	25,44	1
97	20,69	1	22,86	1	27,12	1	23,55	1	24,24	1	26,18	1
98	21,42	1	22,87	1	25,57	1	29,56	1	28,39	1	31,78	1
99	21,81	1	22,19	1	23,77	1	27,17	1	23,47	1	34,75	1
100	21,53	1	23,07	1	22,99	1	26,62	1	28,96	1	28,32	1
101	21,91	1	21,56	1	24,77	1	26,33	1	28,98	1	26,18	1
102	21,2	1	22,98	1	25,11	1	23,68	1	30,84	1	26,33	1
103	21,5	1	23,75	1	25,33	1	25,44	1	21,85	1	26,24	1
104	21,51	1	22,52	1	24,21	1	24,95	1	27,07	1	30,77	1
105	21,67	1	22,77	1	23,77	1	26,36	1	28,48	1	24,66	1
106	21,42	1	22,12	1	24,48	1	26,8	1	22,86	1	35,27	1
107	21,33	1	23,73	1	21,94	1	27,8	1	24,36	1	30,22	1
108	21,56	1	22,74	1	20,45	1	26,01	1	26,06	1	27,74	1
109	21,31	1	23,49	1	21,35	1	24,58	1	29,98	1	25,66	1
110	21,78	1	23,32	1	24,04	1	27,6	1	22,6	1	22,59	1
111	21,34	1	21,97	1	28,5	1	24,72	1	25,5	1	27,5	1
112	21,22	1	22,68	1	24,92	1	23,79	1	25,46	1	27,52	1
113	21,45	1	21,61	1	24,37	1	27,59	1	33,37	1	32,68	1

	A	B	C	D	E	F	G	H	I	J	K	L
114	21,15	1	23,97	1	25,26	1	22,79	1	27,93	1	26,63	1
115	21,56	1	22,16	1	23,77	1	23,01	1	26,1	1	37,01	1
116	21,95	1	20,88	1	24,97	1	22,93	1	26,08	1	22,98	1
117	21,19	1	21,68	1	26,05	1	25,64	1	29,59	1	30,09	1
118	21,55	1	21,95	1	21,8	1	22,99	1	26,2	1	30,92	1
119	21,54	1	20,61	1	22,19	1	23,2	1	30,11	1	30,78	1
120	21,13	1	22,53	1	23,97	1	24,87	1	22,85	1	30,02	1
121	21	1	23,93	1	24,49	1	24,5	1	25,63	1	28,11	1
122	21,51	1	23,66	1	25,72	1	21,25	1	29,9	1	31,68	1
123	21,22	1	23,24	1	23,1	1	25,04	1	26,22	1	29,19	1
124	21,22	1	23,61	1	22,93	1	21,25	1	26,48	1	30,3	1
125	21,49	1	22,65	1	23,59	1	24,94	1	27,61	1	24,63	1
126	21,54	1	23,77	1	23,46	1	22,87	1	30,32	1	33,6	1
127	21,73	1	22,49	1	26,44	1	24,88	1	23,67	1	30,55	1
128	21,78	1	22,27	1	22,64	1	25,44	1	25,74	1	32,56	1
129	21,06	1	23,94	1	24,59	1	24,32	1	25,85	1	36,25	1
130	21,63	1	21,42	1	24,67	1	22,17	1	26,23	1	26,58	1
131	21,56	1	22,86	1	26,36	1	22,85	1	27,5	1	29,83	1
132	21,34	1	21,66	1	26,01	1	24,95	1	26,26	1	32,61	1
133	21,31	1	21,4	1	25,01	1	25,29	1	25,04	1	31,56	1
134	21,31	1	21,6	1	20,45	1	26,24	1	30,98	1	22,55	1
135	21,67	1	22,68	1	23,94	1	24,37	1	29,68	1	29,47	1
136	21,18	1	20,64	1	22,75	1	21,25	1	21,55	1	30,03	1
137	21,35	1	21,04	1	24,45	1	26,44	1	30,73	1	29,98	1
138	20,69	1	23,29	1	29,1	1	24,76	1	31,29	1	30,21	1
139	21,25	1	22,43	1	20,45	1	22,52	1	32,56	1	25,32	1
140	21,32	1	21,1	1	23,99	1	23,75	1	24,15	1	32,72	1
141	21,7	1	22,71	1	21,07	1	25,34	1	31,78	1	31,92	1
142	21,19	1	22,2	1	22,46	1	25,15	1	32,01	1	26,78	1
143	21,68	1	23,14	1	23,71	1	24,7	1	26,52	1	29,35	1
144	20,82	1	21,24	1	23,55	1	25,04	1	24,67	1	32,18	1
145	21,14	1	20,92	1	24,92	1	23,84	1	21,55	1	29,87	1
146	21,83	1	21,99	1	24,79	1	22,06	1	21,55	1	25,49	1
147	21,37	1	22,13	1	21,07	1	26,86	1	25,34	1	31,48	1
148	21,12	1	22,33	1	26,38	1	26,99	1	26,51	1	30,65	1
149	21,4	1	22,52	1	27,14	1	21,97	1	27,41	1	32,49	1
150	21,09	1	22,07	1	23,34	1	23,39	1	24,98	1	22,55	1
151	21,18	1	23,95	1	25,84	1	28,79	1	27,08	1	26,08	1

	A	B	C	D	E	F	G	H	I	J	K	L
151	21,18	1	23,95	1	25,84	1	28,79	1	27,08	1	26,08	1
152	21,2	1	22,65	1	25,31	1	26,87	1	29,81	1	27,47	1
153	21,35	1	23,74	1	21,94	1	21,25	1	28,77	1	26,57	1
154	21,2	1	22,27	1	20,45	1	24,77	1	26,81	1	22,55	1
155	21,79	1	22,29	1	23,11	1	23,5	1	23,2	1	28,32	1
156	21,65	1	22,57	1	23,72	1	25,85	1	31,52	1	32,8	1
157	21,51	1	21,93	1	24,31	1	21,25	1	28,52	1	38,45	1
158	21,53	1	20,35	1	22,63	1	22,23	1	23,43	1	36,31	1
159	21,83	1	22,83	1	22,99	1	27,14	1	28,21	1	28,93	1
160	21,14	1	23,09	1	20,45	1	27,23	1	28,19	1	30,12	1
161	21,68	1	22,49	1	23,09	1	23,08	1	27,2	1	32,89	1
162	21,37	1	21,46	1	25,21	1	25,19	1	24,1	1	32,42	1
163	21,74	1	22,08	1	23,71	1	28,78	1	25,73	1	22,55	1
164	20,9	1	21,71	1	21,73	1	25,94	1	26,27	1	28,97	1
165	21,53	1	23,98	1	24,27	1	26,79	1	26,13	1	35,2	1
166	21,92	1	22,72	1	22,44	1	25,18	1	21,55	1	28,22	1
167	21,48	1	23,03	1	25,62	1	23,96	1	22,92	1	30,93	1
168	21,58	1	22,21	1	24,86	1	26,73	1	34	1	29,29	1
169	21,61	1	23,43	1	24,84	1	21,33	1	28,65	1	22,55	1
170	21,15	1	23,06	1	22,7	1	23,37	1	21,87	1	27,61	1
171	21,37	1	24,26	1	25,92	1	23,82	1	22,4	1	30,31	1
172	20,67	1	22,52	1	23,2	1	24,7	1	34,03	1	28,18	1
173	21,66	1	22,58	1	21,28	1	22,28	1	26,32	1	24,51	1
174	21,28	1	21	1	25,86	1	25,79	1	29,38	1	35,61	1
175	21,33	1	21,29	1	22,45	1	24,26	1	28,46	1	25,49	1
176	21,32	1	22,7	1	24,13	1	27,17	1	28,57	1	26,97	1
177	21,62	1	23,97	1	23,47	1	21,98	1		0	29,21	1
178	21,09	1	22,29	1	24,28	1	22,41	1	25,88	1	22,55	1
179	21,14	1	23,57	1	24,03	1	26,51	1	26,25	1	31,92	1
180	21,3	1	21,61	1	25,78	1	24,16	1	31,13	1	24,75	1
181	21,87	1	21,41	1	23,94	1	21,25	1	24,72	1	32,17	1
182	21,36	1	21,9	1	22,61	1	26,77	1	25,14	1	22,55	1
183	21,49	1	23,1	1	24,72	1	23,97	1	27,94	1	28,16	1
184	20,77	1	21,85	1	24,07	1	29,03	1	27,76	1	25,1	1
185	21,17	1	23,44	1	25,74	1	25,04	1	28,38	1	23,69	1
186	21,41	1	22,8	1	21,88	0	26,09	1	31,86	1	30,57	1
187	21,49	1	22,3	1	25,11	1	24,74	1	26,04	1	23,96	1
188	21,79	1	24,34	1	22,44	1	25,34	1	33,03	1	32,03	1

	A	B	C	D	E	F	G	H	I	J	K	L
166	21,92	1	22,72	1	22,44	1	25,18	1	21,55	1	28,22	1
167	21,48	1	23,03	1	25,62	1	23,96	1	22,92	1	30,93	1
168	21,58	1	22,21	1	24,86	1	26,73	1	34	1	29,29	1
169	21,61	1	23,43	1	24,84	1	21,33	1	28,65	1	22,55	1
170	21,15	1	23,06	1	22,7	1	23,37	1	21,87	1	27,61	1
171	21,37	1	24,26	1	25,92	1	23,82	1	22,4	1	30,31	1
172	20,67	1	22,52	1	23,2	1	24,7	1	34,03	1	28,18	1
173	21,66	1	22,58	1	21,28	1	22,28	1	26,32	1	24,51	1
174	21,28	1	21	1	25,86	1	25,79	1	29,38	1	35,61	1
175	21,33	1	21,29	1	22,45	1	24,26	1	28,46	1	25,49	1
176	21,32	1	22,7	1	24,13	1	27,17	1	28,57	1	26,97	1
177	21,62	1	23,97	1	23,47	1	21,98	1		0	29,21	1
178	21,09	1	22,29	1	24,28	1	22,41	1	25,88	1	22,55	1
179	21,14	1	23,57	1	24,03	1	26,51	1	26,25	1	31,92	1
180	21,3	1	21,61	1	25,78	1	24,16	1	31,13	1	24,75	1
181	21,87	1	21,41	1	23,94	1	21,25	1	24,72	1	32,17	1
182	21,36	1	21,9	1	22,61	1	26,77	1	25,14	1	22,55	1
183	21,49	1	23,1	1	24,72	1	23,97	1	27,94	1	28,16	1
184	20,77	1	21,85	1	24,07	1	29,03	1	27,76	1	25,1	1
185	21,17	1	23,44	1	25,74	1	25,04	1	28,38	1	23,69	1
186	21,41	1	22,8	1	21,88	0	26,09	1	31,86	1	30,57	1
187	21,49	1	22,3	1	25,11	1	24,74	1	26,04	1	23,96	1
188	21,79	1	24,34	1	22,44	1	25,34	1	33,03	1	32,03	1
189	21,4	1	22,19	1	24,01	1	27,41	1	27,52	1	34,06	1
190	21,3	1	23,35	1	24,15	1	25,37	1	26,35	1	37,24	1
191	21,85	1	20,99	1	21,65	1	25,58	1	25,2	1	27,13	1
192	21,16	1	22,67	1	22,71	1	26,14	1	32,43	1	31,94	1
193	21,25	1	22,8	1	21,19	1	26,51	1	22,89	1	30,38	1
194	21,28	1	22,82	1	23,58	1	28,73	0	29	1	30,37	1
195	21,63	1	23,32	1	23,6	1	24,98	1	23,41	1	31,13	1
196	21,61	1	22,66	1	21,92	1	24,36	1	24,51	1	34,8	1
197	21,42	1	22,14	1	25,23	1	26,89	1	25,54	1	28,35	1
198	21,65	1	23,13	1	26,41	1	26,71	1	25,74	1	27,29	1
199	21,16	1	23,95	1	22,85	1	23,2	1	29,22	1	24,6	1
200	21,36	1	22,97	1	22,61	1	23,02	1	26,69	1	27,64	1
201	21,71	1	22,73	1	22,89	0	24,57	1	25,5	1	27,48	1
202	21,47	1	22,77	1	26,05	1	24,71	1	27,58	1	29,47	1

FIGURE 8.3 – Second draft of simulations : 1000 iterations with different numbers of obstacles

8.2.3 A* algorithm : one eVTOL for one target with obstacles

	A	B	C	D	E	F	G	H	I	J	K	L
1	0 obstacle		1 obstacle		2 obstacles		3 obstacles		4 obstacles		5 obstacles	
2	Time	Success	Time	Success	Time	Success	Time	Success	Time	Success	Time	Success
3	21,32	1	21,57	1	21,34	1	21,75	1	23,32	1	23,61	1
4	21,41	1	22,04	1	22,95	1	21,37	1	23,07	1	24,4	1
5	21,1	1	20,91	1	22,61	1	21,93	1	23,92	1	24,14	1
6	21,66	1	21,44	1	20,5	1	21,69	1	23,03	1	24,67	1
7	21,31	1	21,78	1	22,68	1	22,83	1	23,59	1	23,65	1
8	21,46	1	21,9	1	21,74	1	22,24	1	23,05	1	24,94	1
9	21,33	1	21,5	1	22,32	1	22,3	1	23,36	1	23,4	1
10	21,08	1	21,51	1	22,51	1	23,73	1	23	1	23,83	1
11	21,79	1	21,35	1	20,66	1	21,2	1	22,75	1	24,26	1
12	21,31	1	20,96	1	21,34	1	22,65	1	22,05	1	23,05	1
13	21,26	1	21,79	1	22,07	1	22,41	1	22,79	1	24,48	1
14	21,92	1	21,37	1	22,13	1	22,82	1	22,74	1	24,91	1
15	21,56	1	20,77	1	21,93	1	22,05	1	24,46	1	24,97	1
16	21,12	1	20,99	1	20,97	1	21	1	21,67	1	22,89	1
17	21,98	1	21,5	1	22,42	1	21,3	1	22,91	1	24,71	1
18	21,72	1	21	1	21,11	1	21,2	1	22,6	1	25,33	1
19	21,69	1	21,88	1	21,62	1	22,6	1	23,48	1	22,64	1
20	21,42	1	22,51	1	21,58	1	22,35	1	23,78	1	24,05	1
21	21,58	1	21,28	1	21,57	1	22,93	1	22,1	1	23,7	1
22	21,26	1	20,94	1	21,38	1	21,35	1	21,62	1	24,29	1
23	21,7	1	21,44	1	21,49	1	20,94	1	23,97	1	24,14	1
24	21,84	1	21,11	1	22,29	1	22,39	1	21,9	1	24,41	1
25	21,22	1	21,51	1	21,41	1	21,81	1	23,25	1	22,82	1
26	21,19	1	20,94	1	21,98	1	22,06	1	23,68	1	23,07	1
27	21,54	1	22,47	1	22,66	1	23,14	1	23,52	1	24,12	1
28	21,2	1	20,96	1	22,09	1	20,65	1	22,83	1	23,51	1
29	21,58	1	20,99	1	21,64	1	22,39	1	23,26	1	23,56	1
30	21,52	1	22,1	1	21,94	1	23,36	1	23,34	1	23,7	1
31	21,3	1	21,72	1	22,32	1	21,15	1	22,38	1	23,33	1
32	21,7	1	21,07	1	21,39	1	21,18	1	23,6	1	24,03	1
33	21,54	1	22,14	1	22,03	1	23,6	1	23,03	1	23,35	1
34	21,38	1	21,65	1	22,15	1	21,83	1	23,38	1	24,3	1
35	21,65	1	22,18	1	22,04	1	22,59	1	22,91	1	24,78	1
36	21,61	1	21,63	1	20,42	1	20,65	1	22,79	1	23,32	1
37	21,41	1	21,73	1	21,15	1	21,76	1	22,91	1	24,94	1
38	21,96	1	22,13	1	20,59	1	21,65	1	23,53	1	24,16	1
39	21,48	1	21,05	1	21,58	1	20,65	1	23,47	1	24,92	1
40	21,22	1	22,06	1	22,06	1	21,6	1	23,57	1	23,92	1
41	21,09	1	21,61	1	21,74	1	22,79	1	21,71	1	23,98	1
42	21,21	1	21,67	1	21,38	1	22,64	1	23,24	1	24,33	1
43	21,24	1	21,24	1	21,81	1	22,02	1	22	1	23,36	1
44	21,37	1	21,55	1	21,51	1	21,88	1	23,31	1	24,35	1
45	21,42	1	21,52	1	21,52	1	21,81	1	24,19	1	23,87	1
46	21,98	1	22,11	1	22,3	1	22,07	1	21,01	1	24,23	1
47	21,59	1	22,23	1	21,96	1	22,29	1	21,96	1	24,89	1
48	20,94	1	21,1	1	22,07	1	23,1	1	22,19	1	22,79	1
49	21,9	1	21,23	1	21,34	1	21,96	1	24,41	1	24,16	1
50	21,08	1	21,37	1	22,22	1	23,38	1	23,42	1	24,45	1
51	21,54	1	21,59	1	22,57	1	22,45	1	25,55	1	23,37	1
52	21,42	1	21,89	1	21,91	1	21,6	1	22,97	1	23,9	1
53	21,1	1	21,44	1	22,91	1	22,2	1	22,06	1	24,35	1
54	21,39	1	21,26	1	23	1	22,18	1	24,36	1	24,13	1
55	21,57	1	22,09	1	22,37	1	21,29	1	23,72	1	23,87	1
56	21,77	1	21,3	1	21,94	1	22,17	1	21,95	1	24,36	1
57	21,37	1	20,85	1	22,24	1	21,31	1	22,2	1	23,28	1
58	21,18	1	21,05	1	22,47	1	22,55	1	22,56	1	24,06	1
59	21,32	1	20,84	1	22,36	1	23,3	1	23,22	1	23,93	1
60	21,52	1	21,58	1	20,85	1	22,81	1	23,73	1	24,11	1
61	21,41	1	20,76	1	20,46	1	22,36	1	22,7	1	23,27	1
62	21,8	1	21,27	1	22,72	1	22,36	1	23,13	1	26,57	1
63	20,81	1	21,48	1	21,46	1	22,1	1	23,25	1	24,1	1
64	21,27	1	21,31	1	20,91	1	22,46	1	23,02	1	22,21	1
65	21,5	1	20,83	1	20,85	1	22,34	1	23,03	1	25,06	1
66	21,39	1	21,78	1	22,22	1	23,46	1	21,08	1	23,96	1
67	21,52	1	21,79	1	21,42	1	22,25	1	23,11	1	24,03	1
68	21,25	1	22,07	1	21,78	1	21,73	1	23,11	1	24,74	1
69	20,68	1	20,23	1	21,22	1	22,38	1	23,98	1	23,88	1
70	21,46	1	21,38	1	20,68	1	21,9	1	23,51	1	23,85	1
71	21,74	1	20,23	1	22,65	1	22,89	1	23,68	1	25,32	1
72	21,45	1	21,81	1	21,55	1	22,03	1	23,16	1	24,98	1
73	21,16	1	20,89	1	21,54	1	21,79	1	22,81	1	24,64	1
74	21,27	1	21,75	1	21,44	1	24,2	1	23,92	1	22,8	1
75	22,12	1	21,81	1	20,93	1	22,09	1	23,64	1	24,55	1
76	21,58	1	20,97	1	22,26	1	22,23	1	23,59	1	22,58	1
77	21,92	1	21,94	1	21,31	1	21,83	1	23,01	1	24,69	1
78	21,26	1	21,96	1	21	1	23,15	1	24,05	1	25,76	1
79	21,36	1	21,96	1	22,45	1	23,12	1	23,77	1	23,06	1
80	21,95	1	21,38	1	21,62	1	22,31	1	21,93	1	23,75	1
81	21,2	1	20,78	1	22,62	1	23,46	1	23,98	1	24,54	1
82	21,13	1	22,61	1	21,05	1	22,08	1	22,98	1	24,5	1
83	21,49	1	20,85	1	21,36	1	21,85	1	21,85	1	25,06	1
84	21,64	1	21	1	21,92	1	21,03	1	24,79	1	23,78	1
85	21,58	1	21,04	1	22,39	1	22,41	1	22,31	1	24,66	1
86	21,24	1	21,84	1	21,36	1	21,18	1	23,99	1	25,15	1
87	21,79	1	21,2	1	22,04	1	22,07	1	22,11	1	23,98	1
88	21,45	1	21,85	1	21,25	1	22,45	1	21,65	1	22,95	1
89	21,41	1	21,08	1	21,38	1	22,46	1	23,62	1	25,77	1
90	21,52	1	21,2	1	21,65	1	22,5	1	22,18	1	23,93	1
91	21,6	1	20,82	1	21,78	1	22,13	1	22,72	1	24,95	1
92	21,74	1	21,48	1	22,47	1	22,1	1	22,53	1	23,84	1
93	21,66	1	21,37	1	21,08	1	23,13	1	23,28	1	23,64	1
94	21,29	1	22,1	1	21,37	1	21,64	1	23,51	1	24,3	1
95	21,14	1	21,12	1	21,85	1	22,26	1	23,46	1	23,17	1
96	20,95	1	22,4	1	20,52	1	22,73	1	22,54	1	23,15	1
97	20,69	1	20,94	1	21,81	1	20,72	1	21,36	1	25,21	1
98	21,42	1	20,99	1	21,14	1	21,8	1	21,57	1	23,06	1
99	21,81	1	21,01	1	21,56	1	21,16	1	23,42	1	25,13	1
100	21,53	1	21,21	1	21,02	1	22,12	1	22,79	1	22,95	1
101	21,91	1	21,32	1	22,92	1	21,97	1	23,44	1	24,92	1
102	21,2	1	21,8	1	21,48	1	22,02	1	24,15	1	22,24	1
103	21,5	1	20,92	1	22,74	1	22,55	1	21,79	1	22,01	1
104	21,51	1	22,18	1	21,13	1	21,76	1	23,28	1	23,06	1
105	21,67	1	21,88	1	22,25	1	22,39	1	22,22	1	23,47	1
106	21,42	1	21,43	1	22,5	1	21,25	1	24,06	1	24,14	1
107	21,33	1	21,93	1	21,14	1	21,92	1	21,98	1	21,54	1
108	21,56	1	21,81	1	20,97	1	22,31	1	23,51	1	24,75	1
109	21,31	1	21,6	1	21,81	1	22,24	1	24,3	1	23,46	1
110	21,78	1	21,46	1	22,21	1	21,91	1	24,18	1	24,11	1
111	21,34	1	20,64	1	21	1	22,5	1	22,13	1	23,47	1
112	21,22	1	21,28	1	21,45	1	21,47	1	21,65	1	23,6	1
113	21,45	1	20,52	1	21,97	1	21,73	1	23,17	1	24,58	1
114	21,15	1	20,57	1	22,39	1	22,47	1	22,56	1	24,5	1
115	21,56	1	21,74	1	21,77	1	22,26	1	21,88	1	23,87	1
116	21,95	1	22,2	1	22,41	1	20,99	1	20,99	1	23,22	1
117	21,19	1	21,43	1	21,86	1	22,48	1	23,19	1	24,25	1
118	21,55	1	21,56	1	22,15	1	21,85	1	23,3	1	23,54	1
119	21,54	1	21,71	1	22,6	1	22,37	1	21,46	1	22,95	1
120	21,13	1	21,31	1	21,54	1	22,19	1	24,48	1	22,9	1
121	21	1	20,3	1	21,23	1	20,91	1	23,57	1	24,97	1
122	21,51	1	21,97	1	21,93	1	22,28	1	22,14	1	24,2	1
123	21,22	1	21,36	1	22,66	1	23,11	1	23,29	1	22,52	1
124	21,22	1	20,23	1	21,6	1	22,49	1	22,68	1	24,28	1
125	21,49	1	21,83	1	21,43	1	22,31	1	23,66	1	22,15	1
126	21,54	1	22,12	1	21	1	22,88	1	22,61	1	24,11	1
127	21,73	1	20,82	1	22	1	22,58	1	22,26	1	23,23	1
128	21,78	1	21,29	1	20,98	1	22,57	1	24,4	1	24,52	1
129	21,06	1	21,14	1	22,13	1	23,24	1	23,15	1	25,4	1
130	21,63	1	22,14	1	21,78	1	23,26	1	23,25	1	24,81	1
131	21,56	1	21,55	1	22,29	1	21,8	1	22,81	1	23,47	1
132	21,34	1	21,08	1	21,23	1	22,69	1	23,88	1	23,08	1
133	21,31	1	21,08	1	22,35	1	23,02	1	22,58	1	24,53	1
134	21,31	1	21,32	1	22,22	1	22,56	1	22,46	1	23,75	1
135	21,67	1	22,06	1	21,92	1	20,65	1	22,65	1	23,62	1
136	21,18	1	21,81	1	21,71	1	22,42	1	23,69	1	24,4	1
137	21,35	1	22,12	1	21,61	1	21,79	1	23,38	1	24,96	1
138	20,69	1	21,64	1	21,55	1	21,87	1	24,01	1	23,37	1
139	21,25	1	21,4	1	21,21	1	21,87	1	21,23	1	22,84	1
140	21,32	1	21,72	1	21,35	1	22,66	1	24,15	1	22,97	1
141	21,7	1	21,62	1	21,47	1	22,19	1	22,95	1	23,39	1
142	21,19	1	22,19	1	22,21	1	22,49	1	22,64	1	22,23	1
143	21,68	1	21,81	1	21,92	1	21,53	1	24,07	1	23,65	1
144	20,82	1	20,88	1	21,22	1	22,57	1	22,23	1	23,96	1
145	21,14	1	20,6	1	22,56	1	21,51	1	23,49	1	22,71	1
146	21,83	1	20,8	1	21,68	1	20,97	1	23,26	1	24,09	1
147	21,37	1	21,73	1	22,23	1	24,08	1	23,28	1	24,39	1
148	21,12	1	22,08	1	22,05	1	22,53	1	24,44	1	24,36	1
149	21,4	1	22,18	1	21,86	1	22,25	1	22,87	1	22,67	1
150	21,09	1	21,1	1	22,63	1	21,86	1	23,48	1	24,16	1
151	21,18	1	21,02	1	21,56	1	21,67	1	22,15	1	24,31	1
152	21,2	1	22,29	1	22,41	1	21,08	1	22,46	1	24,46	1
153	21,35	1	20,83	1	22,53	1	22,69	1	23,7	1	21,25	1
154	21,2	1	21,05	1	20,92	1	23,39	1	21,32	1	25,12	1
155	21,79	1	21,72	1	22,03	1	20,81	1	24,43	1	24,66	1
156	21,65	1	21,44	1	22,03	1	21,35	1	23,02	1	24,35	1
157	21,51	1	21,79	1	22,51	1	22,53	1	23,58	1	24,62	1
158	21,53	1	21,07	1	22,53	1	23,64	1	22,87	1	21,96	1
159	21,83	1	21,9	1	22,28	1	21,19	1	25,61	1	22,88	1
160	21,14	1	20,99	1	22,36	1	22,86	1	23,12	1	23,51	1
161	21,68	1	22,08	1	22,45	1	22,05	1	23,27	1	23,52	1
162	21,37	1	21,53	1	21,12	1	21,21	1	23,83	1	23,53	1
163	21,74	1	21,42	1	21,78	1	21,2	1	22,19	1	24,66	1
164	20,9	1	21,42	1	21,61	1	22,06	1	22,99	1	22,33	1
165	21,53	1	21,73	1	21,66	1	22,8	1	23,01	1	23,95	1
166	21,92	1	21,5	1	20,86	1	21,63	1	21,86	1	23,1	1
167	21,48	1	22,05	1	21,42	1	22,74	1	25,23	1	21,2	1
168	21,58	1	21,06	1	21,3	1	22,32	1	23,32	1	24,18	1
169	21,61	1	21,13	1	21,29	1	23,97	1	23,03	1	23,22	1
170	21,15	1	21,37	1	21,39	1	22,5	1	23,14	1	24,82	1
171	21,37	1	21,15	1	21,46	1	21,22	1	22,65	1	24,69	1
172	20,67	1	21,31	1	21,49	1	21,98	1	23,35	1	22,82	1
173	21,66	1	21,64	1	21,66	1	21,29	1	21,69	1	24,17	1
174	21,28	1	21,24	1	20,76	1	23,01	1	25,9	1	23,52	1
175	21,33	1	21,89	1	21,16	1	22,26	1	22,65	1	24,46	1
176	21,32	1	21,24	1	21,69	1	22,11	1	23,06	1	23,04	1
177	21,62	1	22,26	1	21,22	1	23,11	1	23,67	1	24,28	1
178	21,09	1	21,65	1	21,86	1	21,23	1	21,62	1	24,68	1
179	21,14	1	20,26	1	22,27	1	21,22	1	23,67	1	24	1
180	21,3	1	21,19	1	21,29	1	22,63	1	22,57	1	24,33	1
181	21,87	1	21,95	1	22,71	1	21,72	1	23,15	1	24,33	1
182	21,36	1	21,5	1	21,48	1	22,47	1	22,55	1	23,98	1
183	21,49	1	20,9	1	21,72	1	22,88	1	23,16	1	22,73	1
184	20,77	1	22,14	1	21,94	1	23,04	1	22,48	1	23,1	1
185	21,17	1	21,07	1	22,56	1	23,2	1	24,08	1	22,04	1
186	21,41	1	20,9	1	21,54	1	22,51	1	22,73	1	24,64	1
187	21,49	1	22,54	1	22,55	1	21,03	1	24,6	1	22,8	1
188	21,79	1	21,81	1	21,02	1	21,02	1	22,69	1	22,81	1
189	21,4	1	21,61	1	21,12	1	22,56	1	23,12	1	26,14	1
190	21,3	1	21,43	1	21,67	1	22,67	1	22,93	1	24,45	1
191	21,85	1	20,87	1	21,84	1	22,92	1	22,72	1	25,07	1
192	21,16	1	21,49	1	21,51	1	21,37	1		0	22,29	1
193	21,25	1	21,65	1	21,48	1	23,49	1	21,81	1	22,97	1
194	21,28	1	21,13	1	21,69	1	22,67	1	23,09	1	24,54	1
195	21,63	1	20,6	1	21,45	1	21,12	1	23,71	1	23,08	1
196	21,61	1	21,84	1	21,58	1	22,62	1	22,3	1	25,17	1
197	21,42	1	20,41	1	21,29	1	22,38	1	22,85	1	22,79	1
198	21,65	1	21,95	1	20,62	1	22,52	1	21,89	1	24,13	1
199	21,16	1	21,31	1	21,99	1	20,65	1	22,82	1	23,29	1
200	21,36	1	21,06	1	22,02	1	22,14	1	24,27	1	25,08	1
201	21,71	1	21,14	1	22,23	1	22,17	1	22,85	1	25,17	1
202	21,47	1	20,35	1	22,09	1	21,38	1	23,38	1	23,86	1
203												

FIGURE 8.4 – Third draft of simulations : 1000 iterations with different numbers of obstacles

8.3 Successful mission examples

- 1 eVTOL with 1 target with 0 obstacle : https://youtu.be/jfi_aHsPtlg
- 1 eVTOL with 1 target with 1 obstacle : https://youtu.be/gD_MKt90nSU
- 1 eVTOL with 1 target with 2 obstacles : https://youtu.be/u_8xzGDCKKQ
- 1 eVTOL with 1 target with 3 obstacles : https://youtu.be/Xo47MeF3JM0
- 1 eVTOL with 1 target with 4 obstacles : https://youtu.be/J3piF7S-FPY
- 1 eVTOL with 1 target with 5 obstacles : https://youtu.be/F_KfLjRETGQ
- Emergency protocol : https://youtu.be/4oaVnXlT12k
- 2 eVTOLs with 2 targets : https://youtu.be/Yu7ge0OCnUI

8.4 Simulation code

GitHub repository : https://github.com/DRACO0410/Internship_EVTOL_simulator